

# Mesozoic thermal history and timing of structural events for the Yukon–Tanana Upland, east-central Alaska: $^{40}\text{Ar}/^{39}\text{Ar}$ data from metamorphic and plutonic rocks

Cynthia Dusel-Bacon, Marvin A. Lanphere, Warren D. Sharp, Paul W. Layer, and Vicki L. Hansen

**Abstract:** We present new  $^{40}\text{Ar}/^{39}\text{Ar}$  ages for hornblende, muscovite, and biotite from metamorphic and plutonic rocks from the Yukon–Tanana Upland, Alaska. Integration of our data with published  $^{40}\text{Ar}/^{39}\text{Ar}$ , kinematic, and metamorphic pressure ( $P$ ) and temperature ( $T$ ) data confirms and refines the complex interaction of metamorphism and tectonism proposed for the region. The oldest metamorphic episode(s) postdates Middle Permian magmatism and predates the intrusion of Late Triassic (215–212 Ma) granitoids into the Fortymile River assemblage (Taylor Mountain assemblage of previous papers). In the eastern Eagle quadrangle, rapid and widespread Early Jurassic cooling is indicated by ~188–186 Ma  $^{40}\text{Ar}/^{39}\text{Ar}$  plateau ages for hornblende from plutons that intrude the Fortymile River assemblage, and for metamorphic minerals from the Fortymile River assemblage and the structurally underlying Nasina assemblage. We interpret these Early Jurassic ages to represent cooling resulting from northwest-directed contraction that emplaced the Fortymile River assemblage onto the Nasina assemblage to the north as well as the Lake George assemblage to the south. This cooling was the final stage of a continuum of subduction-related contraction that produced crustal thickening, intermediate- to high- $P$  metamorphism within both the Fortymile River assemblage and the structurally underlying Lake George assemblage, and Late Triassic and Early Jurassic plutonism in the Fortymile River and Nasina assemblages. Although a few metamorphic samples from the Lake George assemblage yield Jurassic  $^{40}\text{Ar}/^{39}\text{Ar}$  cooling ages, most yield Early Cretaceous  $^{40}\text{Ar}/^{39}\text{Ar}$  ages: hornblende ~135–115 Ma, and muscovite and biotite ~110–108 Ma. We interpret the Early Cretaceous metamorphic cooling, in most areas, to have resulted from regional extension and exhumation of the lower plate, previously tectonically thickened during Early Jurassic and older convergence.

**Résumé :** Nous présentons de nouveaux âges  $^{40}\text{Ar}/^{39}\text{Ar}$  pour de la hornblende, de la muscovite et de la biotite provenant de roches plutoniques et métamorphiques des hautes terres du Yukon–Tanana, en Alaska. L'intégration de nos données à des données publiées d'âges  $^{40}\text{Ar}/^{39}\text{Ar}$ , de cinématique et de  $P$  et  $T$  métamorphiques confirment et précisent l'interaction complexe entre le métamorphisme et la tectonique proposée pour la région. L'épisode métamorphique le plus ancien est plus jeune que le magmatisme du Permien moyen mais il s'est produit avant l'intrusion des granitoïdes du Trias tardif (215–212 MA) dans l'assemblage de Fortymile River (assemblage de Taylor Mountain dans des documents antérieurs). Dans le quadrilatère Eagle est, un refroidissement rapide et répandu, au Jurassique précoce, est indiqué par un palier d'âges  $^{40}\text{Ar}/^{39}\text{Ar}$  ~188 à 186 Ma pour de la hornblende provenant de plutons qui pénètrent l'assemblage de Fortymile River ainsi que pour des minéraux métamorphiques de l'assemblage de Fortymile River et pour l'assemblage structurellement sous-jacent de Nasina. Nous interprétons ces âges de Jurassique précoce comme le résultat d'un refroidissement de contraction à direction nord-ouest qui a mis en place l'assemblage de Fortymile River sur l'assemblage de Nasina au nord ainsi que sur l'assemblage de Lake George au sud. Ce refroidissement a été l'étape finale d'un continuum de contraction relié à la subduction qui a produit un épaississement de la croûte, du métamorphisme à pression intermédiaire à élevée à l'intérieur de l'assemblage de Fortymile River ainsi que dans l'assemblage de Lake George qui lui est structurellement sous-jacent et du plutonisme, au Trias tardif et au Jurassique précoce, dans les assemblages de Fortymile River et de Nasina. Bien que quelques échantillons métamorphiques provenant de l'assemblage de Lake George aient donné des âges de refroidissement  $^{40}\text{Ar}/^{39}\text{Ar}$  indiquant le Jurassique, la plupart ont

Received 18 September 2001. Accepted 5 March 2002. Published on the NRC Research Press Web site at <http://cjcs.nrc.ca> on 11 July 2002.

Paper handled by Associate Editor S. Hanmer.

**C. Dusel-Bacon<sup>1</sup> and M.A. Lanphere.** U.S. Geological Survey, Mail Stop 901, 345 Middlefield Road, Menlo Park, CA 94025, U.S.A.

**W.D. Sharp.** Berkeley Geochronology Center, 2455 Ridge Road, Berkeley, CA 94709, U.S.A.

**P.W. Layer.** Department of Geology and Geophysics, University of Alaska, Fairbanks, AK 99775, U.S.A.

**V.L. Hansen.** Department of Geological Sciences, Southern Methodist University, Dallas, TX 75275–0395, U.S.A.

<sup>1</sup>Corresponding author (e-mail: [cdusel@usgs.gov](mailto:cdusel@usgs.gov)).

donné des âges  $^{40}\text{Ar}/^{39}\text{Ar}$  indiquant le Crétacé précoce : soit la hornblende ~ 135–115 Ma et la muscovite et la biotite ~ 110–108 Ma. Dans la plupart des régions, nous croyons que le refroidissement métamorphique du Crétacé précoce a été causé par une extension régionale et l'exhumation de la plaque inférieure, laquelle avait été épaissie tectoniquement au cours d'une convergence survenue au Jurassique précoce et même avant.

[Traduit par la Rédaction]

## Introduction

The Yukon–Tanana terrane, the largest tectonostratigraphic terrane in the northern North American Cordillera, commonly has been defined as the broad elongate band of heterogeneous metamorphic and igneous rocks that lies between the right-lateral Tintina and Denali fault zones in east-central Alaska and Yukon Territory (Coney et al. 1980). The rocks of the Yukon–Tanana terrane occupy a suspect position in the northern Cordillera, being fault bounded along most of their length and lying between autochthonous or slightly displaced North American strata and outboard allochthonous terranes (Fig. 1).

The Alaskan part of this terrane, primarily exposed in the Yukon–Tanana Upland physiographic province (Wahrhaftig 1965), has been subdivided on the basis of differences in the composition and origin of protoliths, and structural and metamorphic histories of its components (Foster et al. 1985; Nokleberg et al. 1989; Hansen et al. 1991; Dusel-Bacon and Hansen 1992; Hansen and Dusel-Bacon 1998; Dusel-Bacon and Cooper 1999). Kinematic data and  $^{40}\text{Ar}/^{39}\text{Ar}$  metamorphic cooling ages from lineated and foliated metamorphic rocks (i.e., L-S tectonites) in the eastern Yukon–Tanana Upland indicated that the tectonites record multiple deformations and that the different metamorphic fabrics formed at different times (Hansen 1990; Hansen et al. 1991; Hansen and Dusel-Bacon 1998). Integration of the kinematic and  $^{40}\text{Ar}/^{39}\text{Ar}$  data from the Alaska–Yukon border area with data determined further to the west within an extensional gneiss dome complex (Pavlis et al. 1993) resulted in the delineation of the following three major deformational events in time, space, and structural level across the Yukon–Tanana Upland from the Alaska–Yukon border to Fairbanks, Alaska: (1) pre-latest Triassic (>212 Ma) northeast-directed, inferred margin-normal contraction of structurally high oceanic and marginal basin rocks of the Seventymile terrane and Taylor Mountain and Nisutlin assemblages; (2) Early Jurassic (>188–185 Ma) northwest-directed, inferred margin-parallel contraction and imbrication that resulted in juxtaposition of the structurally high, outboard assemblages with parautochthonous continental-margin rocks of the Lake George assemblage; and (3) Early Cretaceous (135–110 Ma) southeast-directed crustal extension that resulted in exposure of the structurally deepest, parautochthonous continental rocks (Lake George assemblage) (Hansen et al. 1991; Dusel-Bacon and Hansen 1992; Hansen and Dusel-Bacon 1998).

Geothermobarometric study of tectonites near the Alaska–Yukon border (Dusel-Bacon and Hansen 1992; Dusel-Bacon et al. 1995) showed that intermediate- to high-pressure ( $P$ ; 7–12 kbar; 1 kbar = 100 MPa) amphibolite-facies metamorphism accompanied both the northeast-vergent deformation of the high-level Taylor Mountain assemblage tectonites and the northwest-vergent deformation shared by tectonites of the Taylor Mountain assemblage and the structurally under-

lying Lake George assemblage. Hansen and her coworkers (Hansen 1990; Hansen et al. 1991; Hansen and Dusel-Bacon 1998) interpreted the first event to represent deformation within a west-dipping (present coordinates) late Paleozoic–Triassic subduction zone; the second event to record Early Jurassic collision of an arc and continental margin assemblage with North American crust; and the third event to reflect Early Cretaceous crustal extension and exhumation of the structurally lowest package. The tectonic model for the first two events is conceptually similar to that proposed for the region by Tempelman-Kluit (1979).

In this paper, we present 40 new  $^{40}\text{Ar}/^{39}\text{Ar}$  ages for hornblende (Hbl), muscovite (Ms), and biotite (Bt) from 29 metamorphic rocks and five plutonic rocks from four different areas within the Yukon–Tanana Upland. We use these ages to expand and refine the temporal constraints for the thermal and deformational history of the central and eastern part of the Yukon–Tanana Upland, and to test the thermotectonic model presented previously and summarized above. Our new  $^{40}\text{Ar}/^{39}\text{Ar}$  ages from five plutons provide an improved understanding of the relationship between plutonism, metamorphism, and deformation within and between the various metamorphic assemblages in the study area. In interpreting the Ar spectra for the metamorphic samples, we consider the potential for argon loss resulting from heating by nearby plutons.

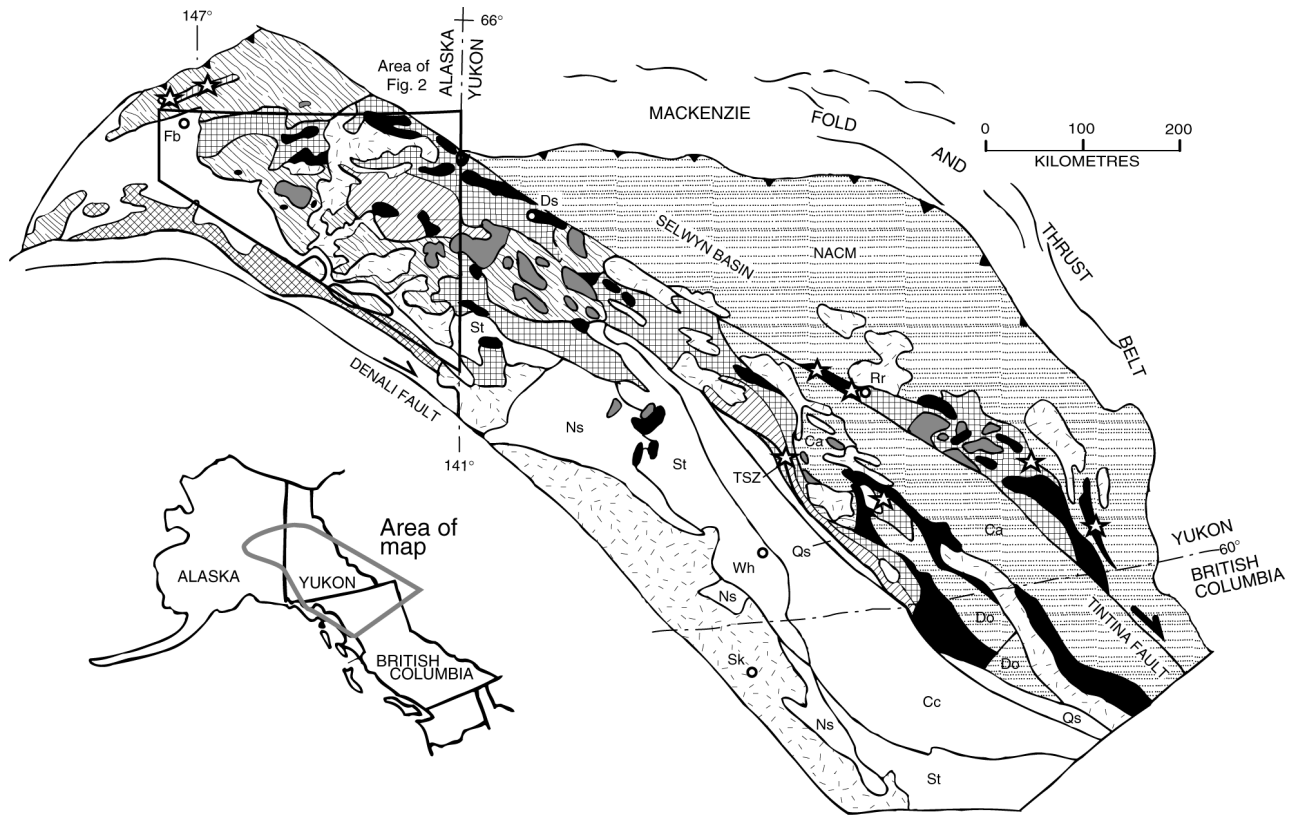
Age divisions used in this paper are those of the Geologic Time Chart presented by Okulitch (1999). Mesozoic Epoch divisions critical to our discussion are the breaks between the Middle and Late Triassic at  $227.4 \pm 4.5$  Ma; the Late Triassic and Early Jurassic at  $200 \pm 1.0$  Ma; and the Early and Middle Jurassic at  $178.0^{+1.0}_{-1.5}$  Ma. Mineral abbreviations used in the text, tables, Appendix A, and figures are those of Kretz (1983) and are listed in Table 1.

## Regional geologic setting

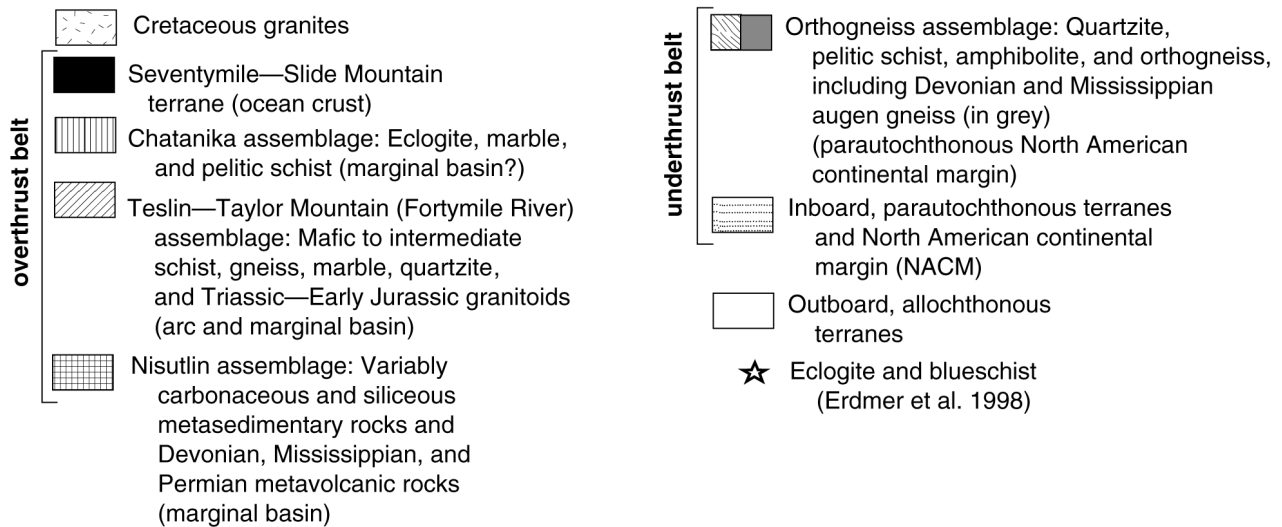
The Yukon–Tanana Upland of east-central Alaska is made up of fault-bounded assemblages of ductilely deformed greenschist- and amphibolite-facies metasedimentary and metaigneous rocks of Paleozoic and Proterozoic(?) protolith age (Dusel-Bacon et al. 1993; Foster et al. 1994; Fig. 2). Late Triassic and Early Jurassic granitoids intrude two of these assemblages in the eastern Yukon–Tanana Upland, and post-kinematic mid-Cretaceous, Late Cretaceous, and early Tertiary granitoids intrude all of the assemblages throughout the upland (Foster 1992). Ductilely deformed rocks are tectonically overlain by weakly metamorphosed oceanic rocks of the Mississippian to Late Triassic Seventymile terrane and are unconformably overlain by Cretaceous and Tertiary volcanic rocks (Foster 1992; Foster et al. 1994).

The structurally lower assemblages (the Lake George assemblage, and the majority of the “ps” and “qq” units of

**Fig. 1.** Simplified terrane and tectonic assemblage map of northern Canadian and Alaskan Cordillera (modified from Hansen et al. (1991), and Dusel-Bacon and Cooper (1999)); data sources listed in those papers). Towns: Ds, Dawson; Fb, Fairbanks; Rr, Ross River; Sk, Skagway; Wh, Whitehorse. Terranes: Ca, Cassiar; Cc, Cache Creek; Do, Dorsey; Ns, Nisling; Qs, Quenellia; St, Stikinia. TSZ, Teslin suture zone. Unlabeled area surrounding Fairbanks is alluvium and unlabeled area adjacent to northern side of Denali fault in Alaska comprises various terranes not discussed in this paper. Tertiary granitoids not shown.



**EXPLANATION**



Foster et al. 1994) consist of amphibolite-facies Qtz–Bt schist and gneiss, pelitic schist, amphibolite, quartzite, and minor marble that were intruded by Devonian peraluminous granitoids, subsequently metamorphosed and deformed to augen gneiss with distinctive white K-feldspar megacrysts (augen) (Fig. 2). A high-grade area of sillimanite gneiss and pelitic schist (Salcha River gneiss dome; Fig. 2) represents a

structural window beneath a low-angle mylonitic shear zone (Dusel-Bacon and Foster 1983), along which lower metamorphic-grade hanging wall rocks moved to the east-southeast relative to footwall rocks (Pavlis et al. 1993).

Several fault-bounded assemblages or terranes overlie the just described amphibolite-facies rocks. The most extensive assemblage comprises the greenschist-facies rocks of the

**Table 1.** Mineral abbreviations used in this paper.

Act	actinolite
Amp	amphibole
Ap	apatite
Atg	antigorite
Bt	biotite
Cal	calcite
Chl	chlorite
Cpx	clinopyroxene
Czo	clinozoisite
Di	diopside
Ep	epidote
Fld	feldspar
Grt	garnet
Hbl	hornblende
Ilm	ilmenite
Kfs	K-feldspar
Ky	kyanite
Mag	magnetite
Ms	muscovite
Opq	opaque oxide
Pl	plagioclase
Qtz	quartz
Rt	rutile
Ser	sericite
Sil	sillimanite
St	staurolite
Stp	stilpnomelane
Ttn	titanite
Wm	white mica
Zo	zoisite
Zrn	zircon

Nisutlin assemblage, in part of Devonian and Mississippian age, which consists of a lower stratigraphic sequence (Nasina assemblage) of carbonaceous quartzite and calcphyllite, and an upper stratigraphic sequence of Qtz-eye semischist, white-mica phyllite, quartzite, marble, and bimodal metavolcanic rocks (Foster et al. 1994; Dusel-Bacon et al. 1993) (Figs. 1, 2). Permian felsic metavolcanic rocks occur in association with carbonaceous rocks just west of the Alaska–Yukon border (Dusel-Bacon et al. 1998). Eclogite-bearing klippe (Chatinika assemblage) overlie the Qtz-rich rocks of unit “qq” northeast of Fairbanks and klippe of the Seventymile terrane occur as scattered remnants across the study area (Foster et al. 1994) (Fig. 2). The Seventymile terrane consists of variably serpentinized peridotite, weakly metamorphosed mafic volcanic rocks, and Mississippian to Late Triassic sedimentary rocks; these rocks are thought to constitute a dismembered ophiolite and its sedimentary cover (Foster et al. 1994).

In the eastern Yukon–Tanana Upland (Fig. 3), the Nisutlin assemblage is structurally overlain by Paleozoic amphibolite-facies rocks, including Grt amphibolite, Bt ± Hbl ± Grt gneiss and schist, marble, quartzite, metachert, pelitic schist (Foster 1976; Hansen et al. 1991), and small bodies of tonalitic orthogneiss (Szumigala et al. 2000b; Day

et al. 2000) and augen gneiss with pink K-feldspar augen. These amphibolite-facies rocks have been referred to previously as the Y4 subterrane of the Yukon–Tanana terrane (Foster et al. 1994), the Teslin–Taylor Mountain terrane (a term proposed by Hansen (1990) to genetically link the rocks in the Taylor Mountain area with similar rocks in the Teslin suture zone in southern Yukon Territory; Fig. 1), the Taylor Mountain terrane (Dusel-Bacon et al. 1995), and most recently, the Taylor Mountain assemblage (Hansen and Dusel-Bacon 1998).

The “Taylor Mountain” moniker was originally chosen to give a general geographic location to the metamorphic assemblage because these rocks are exposed in the vicinity of Taylor Mountain. Unfortunately, because the mountain itself is underlain by undeformed Late Triassic granitoids, discussion of both the Taylor Mountain granitoids and the metamorphic rocks of the “Taylor Mountain assemblage,” an assemblage that extends far beyond the Taylor Mountain area, can be confusing. For this reason, we introduce the new term, “Fortymile River assemblage,” to describe these metamorphic rocks because the rock package is well exposed along the Fortymile River and it underlies most of the Fortymile River drainage in Alaska (Figs. 2, 3, 7). This term harkens back to the assignment of some of these rocks to the “Fortymile series” by Spurr (1898); this term was later abandoned (Mertie 1930). The “Fortymile River assemblage” of this paper is one and the same as the “Taylor Mountain assemblage” (Hansen and Dusel-Bacon 1998) and the “Taylor Mountain terrane” (Dusel-Bacon et al. 1995). A wide, shallowly north-dipping, poorly exposed ductile fault zone (up to as much as 1–2 km of structural thickness) locally separates the Fortymile River assemblage from the underlying Lake George assemblage (Dusel-Bacon et al. 1995; Hansen and Dusel-Bacon 1998).

Both the Nisutlin and the Fortymile River assemblages are intruded by Late Triassic and Early Jurassic granodioritic to syenitic plutons that have Pb isotopic ratios (Aleinikoff et al. 1987) and major and trace element compositions (Newberry et al. 1995a) indicative of an island-arc origin. Previous thermochronology showed that metamorphic rocks from the structurally high assemblages (Fig. 1; most notably the Fortymile River assemblage) yield Late Triassic or Early Jurassic metamorphic cooling ages, whereas rocks from the structurally lower assemblages generally yield Early Cretaceous metamorphic cooling ages (Hansen et al. 1991; Pavlis et al. 1993).

Subsequent to the postulated Early Cretaceous (135–110 Ma) period of regional extension, widespread intrusion of granitoids with trace- and major-element arc signatures occurred throughout the Yukon–Tanana Upland in mid- to Late Cretaceous time (108 to 88 Ma; Wilson et al. 1985; Newberry et al. 1998a). A large caldera complex, just north and east of Tok (Fig. 2), was erupted during this episode at ~93 Ma (Bacon et al. 1990). Within-plate (extensional) felsic magmatism occurred at ~75–65 Ma (Wilson et al. 1985; Newberry et al. 1998b), followed by bimodal within-plate magmatism at ~60–50 Ma (Bacon et al. 1990; Foster et al. 1994; Newberry et al. 1995a). Apatite fission-track ages of ~50–40 Ma indicate that rapid regional cooling and exhumation closely followed Eocene extensional magmatism (Dusel-Bacon and Murphy 2001).

**Fig. 2.** Generalized geologic map showing  $^{40}\text{Ar}/^{39}\text{Ar}$  sample locations. Geology after Dusel-Bacon et al. (1993) and references therein. Additional age information for plutons: Newberry et al. (1998b) and J.K. Mortensen (unpublished data). Areas shown with no pattern are Devonian and Cambrian to Late Proterozoic sedimentary rocks north of the Tintina fault, and Quaternary surficial deposits elsewhere. See text for explanation of assemblage and terrane terminology. Cr., Creek; Fk, Fork.

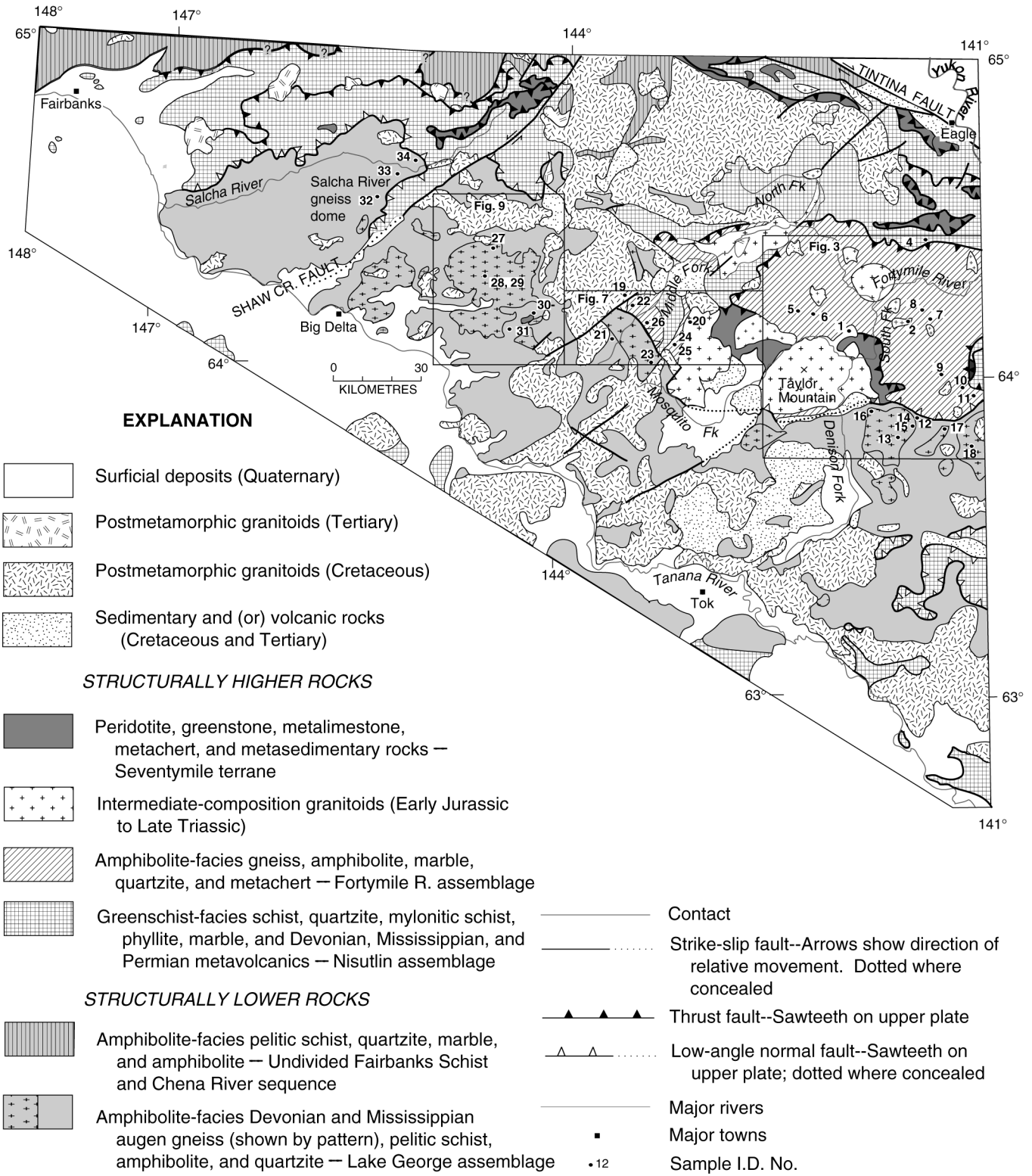


**Fig. 3.** Simplified geologic map of the eastern Eagle–Tanacross area showing  $^{40}\text{Ar}/^{39}\text{Ar}$  ages and kinematic shear sense indicators. Geology modified from Foster (1992) and Szumigala et al. (2000a); kinematic shear-sense indicators from Hansen and Dusel-Bacon (1998). Areas north and south of  $64^\circ$  latitude are located in the southeastern part of the Eagle quadrangle, and the northeastern part of the Tanacross quadrangle, respectively. Map unit patterns as on Fig. 2, except new horizontal-ruled pattern near  $141^\circ$  longitude and  $64^\circ$  latitude represents Permian felsic metavolcanic schist and associated quartzite (Klondike Schist unit as shown on Dusel-Bacon et al. 1998). Rocks shown as Nisutlin assemblage along the northern and eastern edge of Fig. 3 consist of carbonaceous phyllite and quartzite correlative with the Nasina assemblage in Canada. Rocks shown as part of the Seventymile terrane east of the Dennison Fork consist of massive to foliated greenstone, marble, chert, quartzite, dolomite, phyllite, and graywacke (mapped as “Metamorphic rocks of the Chicken area” on Foster 1969) but may not correlate with Seventymile terrane rocks elsewhere in the Yukon–Tanana Upland. Ages (in Ma) are rounded to nearest whole number; age uncertainties are given only for values  $> \pm 3$  Ma.

A series of steep, northeast-striking faults subsequently developed across the Yukon–Tanana Upland (Foster et al. 1994). These faults have been interpreted to have resulted from left-lateral movement and clockwise-rotation of blocks as a result of right-lateral movement along both the Tintina and Denali fault systems that truncate the northern boundary of the Yukon–Tanana Upland and the southern boundary of similar rocks in the northern Alaska Range, respectively, (Page et al. 1995). Unit displacements across the northeast-striking faults indicate both left-lateral and vertical apparent displacement. Apatite fission-track data suggest that up to 3 km of post-40 Ma vertical displacement occurred along some of the northeast-trending faults (Dusel-Bacon and Murphy 2001).

## $^{40}\text{Ar}/^{39}\text{Ar}$ thermochronology

### Sources of data and analytical techniques used

$^{40}\text{Ar}/^{39}\text{Ar}$  analyses were performed on 40 mineral separates from metamorphic or plutonic rocks collected in four different parts of the Yukon–Tanana Upland: the eastern Eagle – Tanacross quadrangles area (Fig. 3), the Molly Creek area (Fig. 7), the Central Creek area (Fig. 9), and the eastern flank of the Salcha River gneiss dome (Fig. 2). Field and petrographic descriptions of the samples and their locations are given in Appendix 1 (Table A1). To simplify discussion, we refer to the samples in the text, tables, appendix, and figures by an I.D. number; corresponding field numbers are also given in Appendix 1, Table 2, Tables D1–D3<sup>2</sup>, and Figs. 5, 8, and 10. Sixteen mineral separates were analyzed by the  $^{40}\text{Ar}/^{39}\text{Ar}$  total fusion method (Table D1). Incremental step-heating experiments were performed on 32 of the mineral separates, including eight that previously had been analyzed by total fusion. Of the separates that were analyzed by incremental step-heating, 26 were heated using a resistance-type furnace (Table D2) and six were heated by a laser (Table D3).

For this paper, we have adopted the following plateau criteria: at least 3 consecutive fractions constituting at least 50% of the  $^{39}\text{Ar}$  release and for which no difference in age can be detected between any two fractions at the 95% confidence level as defined by a mean square of weighted deviates (MSWD) significant at the 95% confidence level (Fleck et al. 1977, calculated using the ISOPLOT program of Ludwig 2000). Age spectra with plateau-like segments, but not meeting these criteria (e.g., less than 3 fractions, higher than

expected MSWD) are termed “pseudoplateaus” and the quoted error for these has been modified by the square root of MSWD to reflect the scatter in the fraction ages. Error uncertainties in our reported ages are at the 1s level. Ar release spectra reveal plateau or pseudoplateau ages for 26 of the separates (Figs. 5, 8, 10). The remaining six determinations did not show plateau-like segments. A summary of the  $^{40}\text{Ar}/^{39}\text{Ar}$  age determinations and a reference for the protocol of the analytical techniques used on each sample are given in Table 2.

To place ages from the different laboratories on a consistent basis, all ages were calculated relative to an age of 27.92 Ma for sanidine from the Taylor Creek rhyolite (Duffield and Dalrymple 1990; = 27.60 Ma age for Fish Canyon tuff sanidine). Although this has the desirable effect of making the  $^{40}\text{Ar}/^{39}\text{Ar}$  data internally consistent, recent evidence suggests that this standardization may yield  $^{40}\text{Ar}/^{39}\text{Ar}$  ages that are systematically 2–3% younger than U–Pb zircon ages (Min et al. 2000). In discussing the cooling history of our  $^{40}\text{Ar}/^{39}\text{Ar}$  samples, we assume the following closure temperatures:  $450 \pm 50^\circ\text{C}$  for hornblende (Baldwin et al. 1990);  $375 \pm 25^\circ\text{C}$  for muscovite (Hunziker et al. 1992); and  $300 \pm 50^\circ\text{C}$  for biotite (Harrison et al. 1985).

All of the metamorphic mineral samples we analyzed are from rocks whose mineralogy and penetrative fabrics indicate metamorphism in a mid-crustal, dynamothermal environment. However, given the presence of many large granitoid plutons in the region, we considered the potential for a subsequent reset of the Ar systematics by conductive heat transfer from nearby plutons. We examined the Qtz fabric in thin sections of our samples for evidence of either dynamothermal crystallization or static recrystallization (annealing) that would indicate a thermal overprint, presumably from nearby plutons. Microtextural evidence in Qtz grains for intracrystalline deformation during dynamothermal metamorphism includes undulose extinction and irregular (ragged) grain or subgrain boundaries, whereas evidence for static recrystallization includes straight, often  $120^\circ$ , grain-boundary intersections and uniform extinction (e.g., Passchier and Trouw 1996). Quartz grains in samples 5 and 17 have primarily straight grain boundaries and uniform extinction, but all other samples have some degree of undulose extinction and ragged, irregular grain or subgrain boundaries (Appendix 1), indicative of intracrystalline strain. We also considered distance of  $^{40}\text{Ar}/^{39}\text{Ar}$  samples from nearby plutons. Lacking the information necessary for thermal mod-

<sup>2</sup>Complete data tables may be purchased from the Depository of Unpublished Data, CISTI, National Research Council of Canada, Ottawa, ON K1A 0S2, Canada.



**Table 2.** Summary of  $^{40}\text{Ar}/^{39}\text{Ar}$  ages, method of analysis, laboratory used, and reference for description of laboratory protocol.

Sample ID No.	Rock type	Meta. assem. <sup>a</sup>	Mineral dated	Plateau age <sup>b, c</sup>	Plateau details	Integrated age <sup>c</sup>	Total fusion age <sup>d</sup>
1	Qtz monzonite		Hbl	187.0 ± 0.5 (PL) (pseudoplateau)	2 fractions, 71% $^{39}\text{Ar}$ release, MSWD = 0.4	185.4 ± 0.5 (PL)	
1	Qtz monzonite		Bt		None	182.6 ± 0.5 (PL)	
2	Hbl monzonite		Hbl	186.6 ± 1.0 (ML)	9 fractions, 100% $^{39}\text{Ar}$ release, MSWD = 1.1		
3	Hbl–Cpx monzodiorite		Hbl	188.1 ± 1.4 (PL-las) (pseudoplateau)	6 fractions, 81% $^{39}\text{Ar}$ release, MSWD = 5.0	188.6 ± 0.7 (PL-las)	
4	Wm quartzite/ exhalite with banded sulfides	Nas.	Ms	181.7 ± 0.9 (fine-grained, 250–500 µm fraction) (PL-las)	11 fractions, 95% $^{39}\text{Ar}$ release, MSWD = 0.6	181.8 ± 0.9 (PL-las)	
4	Wm quartzite/ exhalite with banded sulfides	Nas.	Ms	182.9 ± 0.5 (coarser-grained, 500–1000 µm fraction) (PL-las)	5 fractions, 53% $^{39}\text{Ar}$ release, MSWD = 1.5	191.9 ± 0.6 (PL-las)	
5	Grt Qtz mica schist	FMR	Bt	184.9 ± 1.2 (WS)	8 fractions, 55% $^{39}\text{Ar}$ release, MSWD = 0.4	179.9 ± 0.8 (WS)	181.6 ± 0.9
6	Hbl–Bt–Grt schist	FMR	Bt	176.7 ± 1.0 (WS)	6 fractions, 56% $^{39}\text{Ar}$ release, MSWD = 0.6	172.2 ± 1.1 (WS)	174.7 ± 2.2
7	Grt–St Qtz mica schist	FMR	Bt				185.6 ± 0.4
8	Mylonitic Bt augen gneiss	FMR	Bt	190.4 ± 1.8 (PL-las)	3 fractions, 56% $^{39}\text{Ar}$ release, MSWD = 0.2	180.3 ± 2.1 (PL-las)	
9	Hbl schist	FMR	Hbl				186.2 ± 1.3
10	Grt amphibolite	FMR	Hbl				202.4 ± 1.6
11	Qtz–Zo–Bt–Ms gneiss	FMR?	Ms	176.8 ± 0.9 (ML)	7 fractions, 64% $^{39}\text{Ar}$ release, MSWD = 0.8	176.8 ± 0.9 (ML)	
11	Qtz–Zo–Bt–Ms gneiss	FMR	Bt	123.6 ± 0.7 (ML), pseudoplateau	12 fractions, 81% $^{39}\text{Ar}$ release, MSWD = 5.9	119.4 ± 0.5 (ML)	
12	Hbl–Bt–Ky–Grt schist	LG?	Bt	165.6 ± 0.8 (ML), pseudoplateau	13 fractions, 100% $^{39}\text{Ar}$ release, MSWD = 5.4	165.6 ± 0.8 (ML)	
13	Amphibolite	LG	Hbl	117.6 ± 1.2, pseudoplateau (isochron age = 119.2 ± 0.8) (MH)	22 fractions, 97% $^{39}\text{Ar}$ release, MSWD = 17		
14	Grt–Qtz–Amp schist	LG	Hbl				105.7 ± 1.3
15	Ms–Bt augen gneiss	LG	Ms				108.0 ± 0.3
16	Ms–Bt augen gneiss	LG	Ms	107.5 ± 0.6 (PL-las)	12 fractions, 99% $^{39}\text{Ar}$ release, MSWD = 0.7		
16	Ms–Bt augen gneiss	LG	Bt	110.3 ± 1.1 (PL-las)	5 fractions, 62% $^{39}\text{Ar}$ release, MSWD = 2.2		
17	Bt–Ms augen gn	LG	Ms				110.6 ± 0.7
17	Bt–Ms augen gn	LG	Bt				107.6 ± 0.3
18	Bt–Hbl augen gneiss	LG	Bt				107.8 ± 0.3
19	Bt–Hbl Qtz monzonite		Bt	106.7 ± 0.6 (ML)	12 fractions, 98% $^{39}\text{Ar}$ release, MSWD = 0.7	106.7 ± 0.6 (ML)	
20	Qtz monzonite		Hbl	179.1 ± 1.1 (ML)	10 fractions, 99% $^{39}\text{Ar}$ release, MSWD = 0.3	179.1 ± 1.1 (ML)	

21	Qtz mica schist	LG	Ms	108.4 ± 0.6 (WS)	13 fractions, 96% <sup>39</sup> Ar release, MSWD = 0.3	108.5 ± 0.5 (WS)	
22	Grt–Chl–Wm–Qtz schist	FMR	Ms	complex spectrum (WS)	None	136.8 ± 0.8 (WS)	138.8 ± 0.8
23	Hbl–Ep–Qtz schist	FMR	Hbl	complex spectrum (WS)	None	168.6 ± 2.1 (WS)	
24	Ms–Qtz schist	FMR	Ms	174.8 ± 4.7 (WS), pseudoplateau	slightly concave spectrum (WS), 14 fractions, 92% <sup>39</sup> Ar release, MSWD = 12	173.4 ± 1.0 (WS)	171.6 ± 0.7
25	Grt amphibolite	FMR	Hbl	complex spectrum (WS)	None	157.6 ± 2.8 (WS)	153.4 ± 5.8
26	Ms–Qtz–Grt–Zo–Chl schist	LG	Ms	complex spectrum (WS)	None	197.9 ± 1.0 (WS)	199.8 ± 2.0
27	Amphibolite	LG	Hbl	135.3 ± 3.2 (ML), pseudoplateau	9 fractions, 94% <sup>39</sup> Ar release, MSWD = 4.1	135.3 ± 1.4 (ML)	
28	Grt amphibolite	LG	Hbl	181.0 ± 6.5 (ML)	6 fractions, 84% <sup>39</sup> Ar release, MSWD = 2.4		
29	Hbl–Bt–Pl schist	LG	Hbl	130.4 ± 1.1 (ML), pseudoplateau	2 fractions 43% <sup>39</sup> Ar release, MSWD = 0.0		
30	Amphibolite	LG	Hbl	120.4 ± 0.7 (WS)	6 fractions, 82% <sup>39</sup> Ar release, MSWD = 0.6	118.9 ± 1.2 (WS)	120.2 ± 0.7
31	Grt–St–Ky Qtz mica schist	LG	Ms	108.3 ± 0.6 (WS)	4 fractions, 54% <sup>39</sup> Ar release, MSWD = 1.2	107 ± 0.8 (WS)	112.6 ± 1.5
32	Hbl–Pl–Bt schist	LG	Hbl	113.6 ± 2.8 (ML)	9 fractions, 98% <sup>39</sup> Ar release, MSWD = 1.2		
32	Hbl–Pl–Bt schist	LG	Bt	109.3 ± 0.6 (ML)	9 fractions, 68% <sup>39</sup> Ar release, MSWD = 0.9		
33	Hbl–Bt–Pl–Qtz schist	LG	Hbl	complex spectrum (ML)	None		
34	Qtz–Ms schist	LG	Ms	109.6 ± 0.6 (ML)	8 fractions, 95% <sup>39</sup> Ar release, MSWD = 1.0		

<sup>a</sup>Abbreviations for metamorphic assemblage (Meta. assem.) of sample: Nas., Nasina; FMR, Fortymile River; LG, Lake George.

<sup>b</sup>All ages meet our criteria for a plateau, unless indicated below to be a pseudoplateau (see text for criteria and explanation).

<sup>c</sup>Abbreviations for laboratory in which incremental <sup>40</sup>Ar/<sup>39</sup>Ar step-heating experiment was conducted and reference for laboratory protocol. Furnace step heating: ML, Marvin Lanphere (Lanphere 2000); WS, Warren Sharp (Sharp et al. 1996, 2000); PL, Paul Layer, (Newberry et al. 1998b); MH, Mark Harrison (Harrison and Fitzgerald 1986). Single-grain laser step heating: PL-las, Paul Layer (Newberry et al. 1998b; Layer 2000). Complete data are given in depository Tables D2 and D3. These may be purchased from the Depository of Unpublished Data, CISTI, National Research Council of Canada, Ottawa, ON K1A 0S2, Canada.

<sup>d</sup>All <sup>40</sup>Ar/<sup>39</sup>Ar total fusion age determinations were made by Marvin Lanphere; see Dalrymple (1989) for laboratory protocol. Complete data are given in depository Tables D1. These may be purchased from the Depository of Unpublished Data, CISTI, National Research Council of Canada, Ottawa, ON K1A 0S2, Canada.

**Fig. 4.** Photograph of intensely deformed augen gneiss (location of sample I.D. No. 16, Fig. 3) within the ductile fault zone separating the Lake George and Fortymile River assemblages. Tectonic transport direction (shown by K-feldspar augen) is top-to-the-northwest (left in photo).



eling (such as the temperature, shape, and depth of the plutons; the method of heat transfer; the extent of fluid flow; the temperature of the wall rocks; etc.), we assume, for discussion purposes, the simplistic view that the thermal effects from the nearby granitoid plutons adequate to reset Ar systematics in the wall rocks are more likely within a distance equal to the radius of a spherical pluton or half of the width of a tabular or sheet-like body and are increasing less likely with increasing distance from the pluton. We discuss the potential for thermal resetting only for those samples for which a thermal reset by nearby plutons is likely based on either proximity to plutons or textural evidence.

### Eastern Eagle – Tanacross area

#### Geologic setting

Our most detailed thermochronometric analysis focuses on the southeastern Eagle and northeastern Tanacross quadrangles (Fig. 3), an area that has a low volume of Cretaceous granitoids, is locally well exposed, and is traversed by the Taylor Highway. Mafic gneiss and schist, marble, quartzite, metachert, and pelitic schist of the Fortymile River assemblage dominates the area; the Seventymile terrane and Nisutlin assemblage are exposed to the north, east, and west, and the Lake George assemblage is exposed to the south. Late Triassic and Early Jurassic plutons are abundant in the Fortymile River assemblage but do not occur in the structurally underlying Lake George assemblage.

Peraluminous augen gneiss is the dominant lithology in the Lake George assemblage south of the north-dipping ductile fault zone that separates this assemblage from quartzite, marble, and amphibolite of the Fortymile River assemblage (Foster 1992; Dusel-Bacon and Hansen 1992). Within the fault zone, rocks of either assemblage may occur, and rocks record northwest-vergent, and locally southeast-vergent shear, and intermediate- to high-*P* amphibolite-facies conditions (Hansen et al. 1991; Dusel-Bacon et al. 1995; Hansen and Dusel Bacon 1998). White K-feldspar augen at one locality along the fault zone (locality from which sample 16 was collected; Fig. 3) have been deformed into ribbons with an ~1:12 length:width ratio (Fig. 4). Well-developed S-C fabrics in peraluminous augen gneiss at this augen “ribbon” locality indicate top-to-the-northwest shear. This fabric was

subsequently deformed into tight, northeast-trending folds whose asymmetry indicates top-to-the-southeast shear. South of the fault zone, top-to-the-northwest shear dominates in the northern, structurally higher part of the Lake George assemblage, and top-to-the-southeast shear dominates in the southern, structurally lower part of the assemblage. Although no sharp division is observed between domains of opposite shear, discreet top-to-the-southeast shear bands cut, and are therefore younger than, more penetratively developed top-to-the-northwest fabrics (Hansen and Dusel-Bacon 1998).

Light gray to black, carbonaceous greenschist-facies Qtz phyllite and Qtz-mica schist of the Nasina assemblage (a subdivision of the Nisutlin assemblage) crop out north of the amphibolite-facies Fortymile River assemblage. Permian metarhyolite occurs within the Nasina assemblage just west of the Alaska–Yukon boundary (Dusel-Bacon et al. 1998). The contact between the Fortymile River and Nisutlin assemblages is interpreted as a complex 1–3 km wide, east-southeast-striking, north-vergent thrust zone (Foster et al. 1985). As originally mapped by Foster (1976), at least part of the contact is a straight, steep, northeast-trending fault (Fig. 3), a common orientation of regionally extensive post-Tertiary faulting (Newberry et al. 1995b).

#### Description of Ar release spectra

##### Jurassic plutonic samples

Hornblende from a sample of Qtz monzonite (sample 1) of the Chicken pluton (Szumigala et al. 2000a), near the northeastern margin of the Taylor Mountain batholith, gives a pseudoplateau age of  $187.0 \pm 0.5$  Ma (Fig. 5A). Biotite separated from the same sample does not give a plateau (Fig. 5B) and has a slight “hump-shape” in the Bt age spectrum, likely due to very minor alteration of the Bt to Chl, observed during petrographic analysis (Appendix 1). Older Early Jurassic  $^{40}\text{Ar}/^{39}\text{Ar}$  plateau ages of  $191 \pm 2$  Ma on Hbl and  $196 \pm 2$  Ma on Bt were determined for a sample of Bt–Hbl Qtz diorite from the Chicken pluton, two km to the east of our sample (Fig. 3; Szumigala et al. 2000a). These older ages were determined using the laser heating method as opposed to the furnace heating method used on our sample 1. Sample 2, a Hbl monzonite from the Napoleon Creek pluton (Szumigala et al. 2000b), yields a well-defined Hbl plateau age of  $186.6 \pm 1.0$  (Fig. 5C). Hornblende separated from Hbl–Cpx monzodiorite sample 3 yields a pseudoplateau age of  $188.1 \pm 1.4$  Ma (Fig. 5D). Sample 3 was collected from the interior of a large batholith, whose map outline (Foster 1976) resembles the shape of a pig’s head, and hence we informally refer to it as the “Pig pluton.” As with the Chicken pluton, an older Hbl  $^{40}\text{Ar}/^{39}\text{Ar}$  plateau age of  $194 \pm 2$  Ma age was determined for the Pig pluton by single-grain laser fusion methods (Szumigala et al. 2000a).

Farther west (Fig. 3), the Mount Warbelow pluton gives a  $^{40}\text{Ar}/^{39}\text{Ar}$  Bt plateau age of  $185 \pm 1$  Ma (Szumigala et al. 2000a) and a  $191.4 \pm 0.4$  Ma Zrn U–Pb age (J.K. Mortensen, oral communication, 2001).

##### Nasina assemblage sulfide-bearing exhalite

Sample 4 is from light-tan, rusty-weathering, sphalerite-, galena-, and celsian-bearing Ms “quartzite” that occurs as an elongate area (original layer?) within a borrow pit of carbo-

naceous Qtz phyllite near the intersection of the steep north-east-trending fault and the inferred south-dipping thrust fault that separates the Nasina assemblage from the higher metamorphic-grade Fortymile River assemblage to the south. The occurrence of celsian (a barium feldspar) and base-metal sulfides is consistent with a hydrothermal (sedimentary exhalative) origin for the “quartzite” (Dusel-Bacon et al. 1998).  $^{40}\text{Ar}/^{39}\text{Ar}$  incremental step-heating by laser was performed on Ms from two different size fractions of sample 4. The finer grained sized fraction (250–500  $\mu\text{m}$ ) has a well-defined plateau age of  $181.7 \pm 0.9$  Ma for 11 fractions and 95% of gas release; we interpret this as the closure of the sample (Fig. 5E). The coarser grained sized fraction (500–1000  $\mu\text{m}$ ) has a plateau age of  $182.9 \pm 0.5$  Ma, defined by 5 fractions and 53% of gas release (Fig. 5F). There is evidence of older ages at both low- and high-temperature steps that may be due to excess Ar and older inclusions, respectively. It is possible that the coarser Ms grains retain some “inherited” (detrital?) pre-metamorphic component.

#### *Fortymile River assemblage metamorphic samples*

Garnetiferous schist was collected for  $^{40}\text{Ar}/^{39}\text{Ar}$  analysis from two separate localities southeast of the Mount Warbelow pluton (Fig. 3). Sample 5 is a Grt–Bt–Qtz–Ms schist with textural features (Appendix 1) that are consistent with static thermal metamorphism superimposed on a penetratively developed fabric. These features include the predominance of uniform extinction and straight grain boundaries in Qtz, and Bt that occurs both as foliation-forming grains and as more coarsely crystalline and randomly oriented crystals within the foliation plane; sericitization of foliation-forming Ms also may be due to static thermal metamorphism. Biotite from sample 5 yields a plateau age of  $186.3 \pm 1.6$  Ma (Fig. 5G). Sample 6, a Grt–Qtz–Bt–Hbl schist, contains fresh Hbl and Bt, but a compositionally similar schist from the same field location contains retrograde Chl around Grt rims and after Bt. Biotite from sample 6 gives a  $^{40}\text{Ar}/^{39}\text{Ar}$  plateau age of  $176.7 \pm 1.0$  Ma (Fig. 5H).

Although sample 5 is beyond the expected thermal effects from the nearby Mount Warbelow pluton and more proximal, smaller bodies, its texture suggests that static thermal metamorphism did, in fact, occur in the area, perhaps explaining the closeness between the Bt cooling ages of the pluton and sample 5. Sample 6, while beyond the expected thermal effects from the nearby Mount Warbelow pluton, it is near a magnetic high (Alaska Division of Geological and Geophysical Surveys 1999) that may be an apophysis of the pluton. Alternatively, the possible reset of Ar data for sample 6 Bt, shown by the four lowest temperature steps, and retrograde alteration in another sample at the locale, may have been related to fluids focussed along the nearby fault mapped by Foster (1976) < 1 km to east; however, this is highly speculative because the age of faulting is unknown.

Farther east, Bt from sample 7, a Grt–St-bearing Qtz–Ms–Bt schist, gives a total fusion age of  $185.6 \pm 0.4$  Ma, and Bt from a pink K-feldspar blastomylonitic augen gneiss (sample 8) has a hump-shaped spectrum with young ages at low- and high-temperature steps. Sample 8 yields a plateau age of  $190.4 \pm 1.8$  Ma for three fractions and 56% of gas release (Fig. 5I). Although the “hump shape” is usually indicative of alteration of the minerals, petrographic examination revealed

no alteration of the Bt but considerable mylonitization and recrystallization resulting in a bimodal grain size and probable replacement of original K-feldspar megacrysts with aggregates of annealed K-feldspar and Qtz. Quartz grains in the matrix, however, have strongly developed undulose extinction and ragged margins.

Total fusion  $^{40}\text{Ar}/^{39}\text{Ar}$  ages were determined for Hbl from two penetratively deformed Hbl-bearing rocks of the Fortymile River assemblage that crop out south of Walker Fork (Fig. 3). At the first locality, highly sheared Hbl–Bt–Chl–calcite–Pl schist (sample 9) yields a  $186.2 \pm 1.3$  Ma total fusion age. Petrographic examination of the dated sample indicates that the pale-green Hbl porphyroblasts form augen-like clasts that are enveloped by through-going folia of Chl, Cal, sericitized Pl, and, locally, chloritized Bt, indicative of recrystallization and shearing under greenschist-facies conditions (Appendix 1). Microprobe analysis of the Hbl separate shows the Hbl to have a homogeneous composition and to be lower in  $\text{Al}_2\text{O}_3$  (10.36 wt.%) than the other  $^{40}\text{Ar}/^{39}\text{Ar}$  Hbl separates from the Fortymile River assemblage, as well as lower than the  $\text{Al}_2\text{O}_3$  values from high-pressure (8–12 kbar) Hbl in amphibolites from the same region (Dusel-Bacon et al. 1995). Although sample 9 is located only 1.2 km from the margin of a small (~1.5 km radius), undated granitoid of probable Early Jurassic age, there is no petrographic evidence to suggest that the sample was affected by static thermal metamorphism. At the second locality, Hbl from a Grt amphibolite (sample 10) that clearly crystallized under higher temperature (amphibolite-facies) conditions, gives an Early Jurassic total fusion age of  $202.4 \pm 1.6$  Ma.

Five miles to the southeast and closer to the fault zone between the Fortymile River and Lake George assemblages (Fig. 3), incremental heating experiments performed on a sample of Qtz–Zo–Bt–Ms gneiss (sample 11) show the complexity of the thermal and deformational history near the tectonic interface between the two assemblages. Muscovite separated from the gneiss yields an undisturbed, flat age spectrum with a plateau age of  $176.8 \pm 0.9$  Ma (Fig. 5J), whereas Bt from the same sample yields a spectrum with a slight variation among individual step ages and a pseudoplateau age of  $123.6 \pm 0.7$  Ma (Fig. 5K). Backscatter electron imaging of a thin section of the sample (Fig. 6A) shows the Ms and Bt to be part of the same penetrative metamorphic fabric and each phase to be homogeneous. We, therefore, conclude that both minerals formed at the same time and that the sample cooled through the closure temperature for Ar diffusion in Ms (~375°C) at ~177 Ma but remained above the closure temperature for Ar diffusion in Bt (~300°C) prior to about 124 Ma. An alternative explanation of the discordancy of the mica ages is that static thermal metamorphism associated with Cretaceous plutons reset the Bt, but the temperature was inadequate to reset the Ms. We consider this possibility to be unlikely because the nearest exposed Cretaceous intrusion (Crag Mountain pluton, to the south;  $107.5 \pm 1$  Ma U–Pb monazite crystallization age, J.K. Mortensen, oral communication, 2001) is far enough away (6.5 km) that no contact effect would be expected, and there is no textural evidence for superimposed static thermal metamorphism in sample 11 and associated rocks.

$^{40}\text{Ar}/^{39}\text{Ar}$  incremental heating experiments were also performed on Bt separated from a Grt–Bt–Ky–Hbl schist (sam-

**Fig. 5.** Ar release spectra for samples from the southeastern Eagle – Tanacross area. Box heights of each rectangle are  $\pm 1s$ .

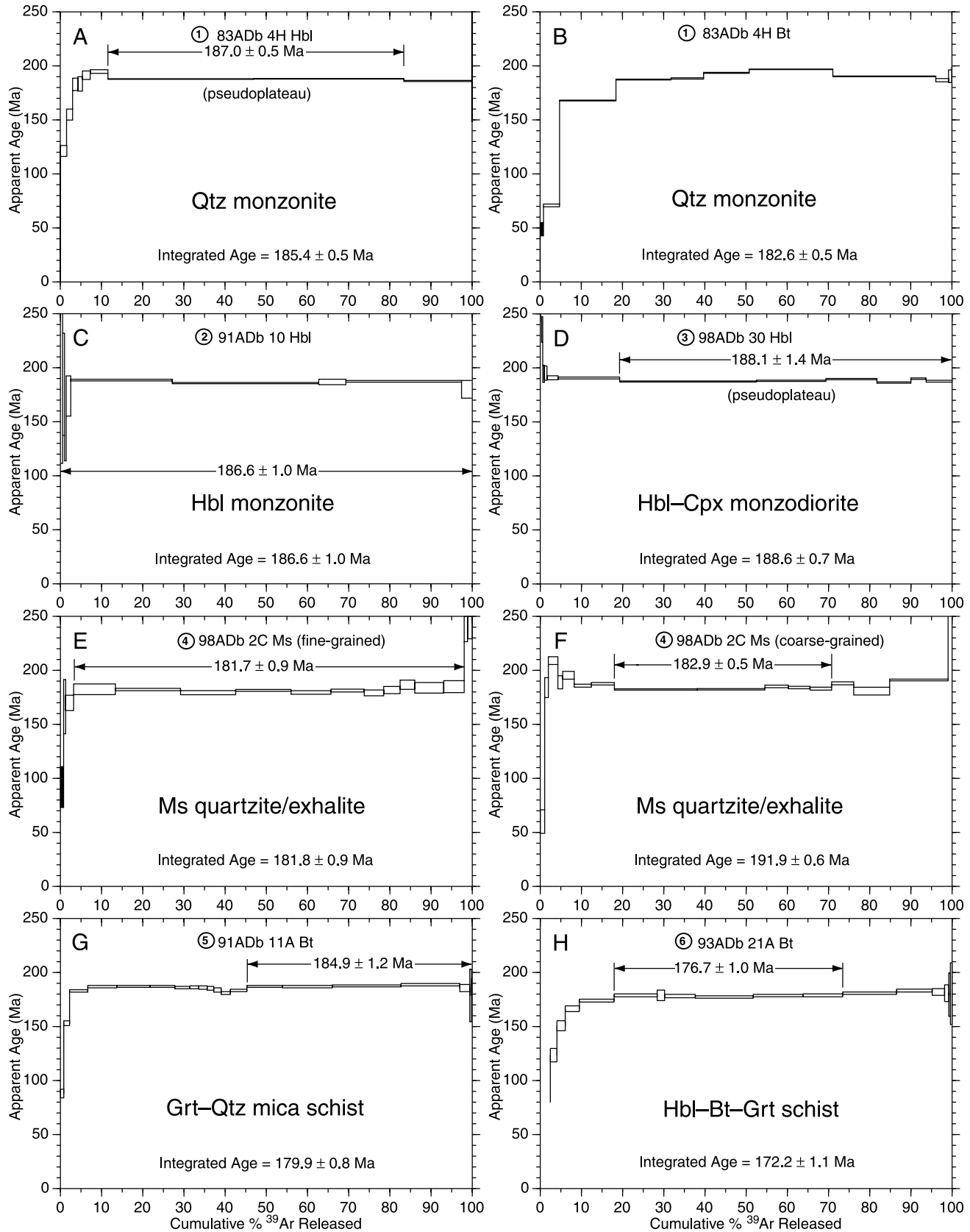
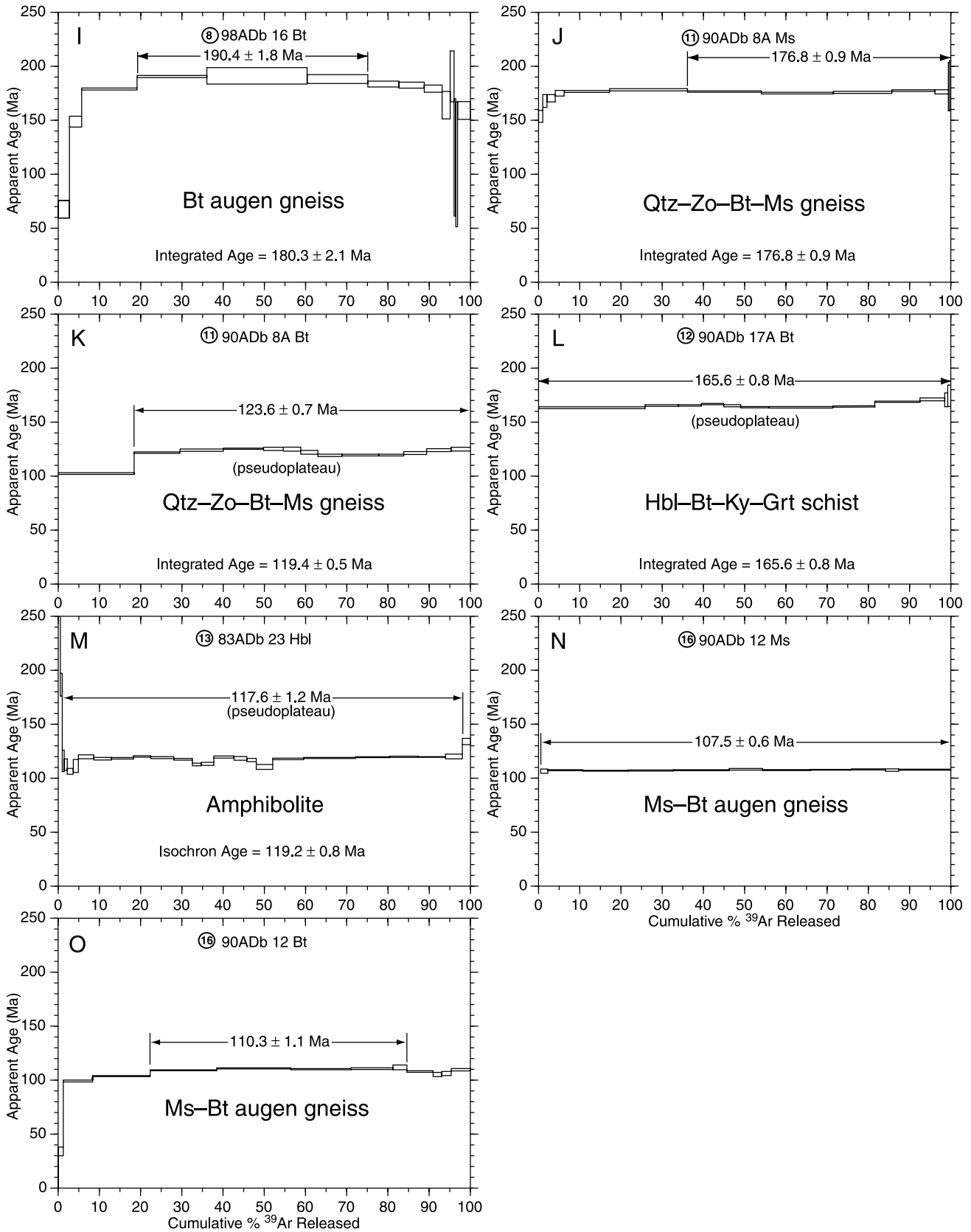
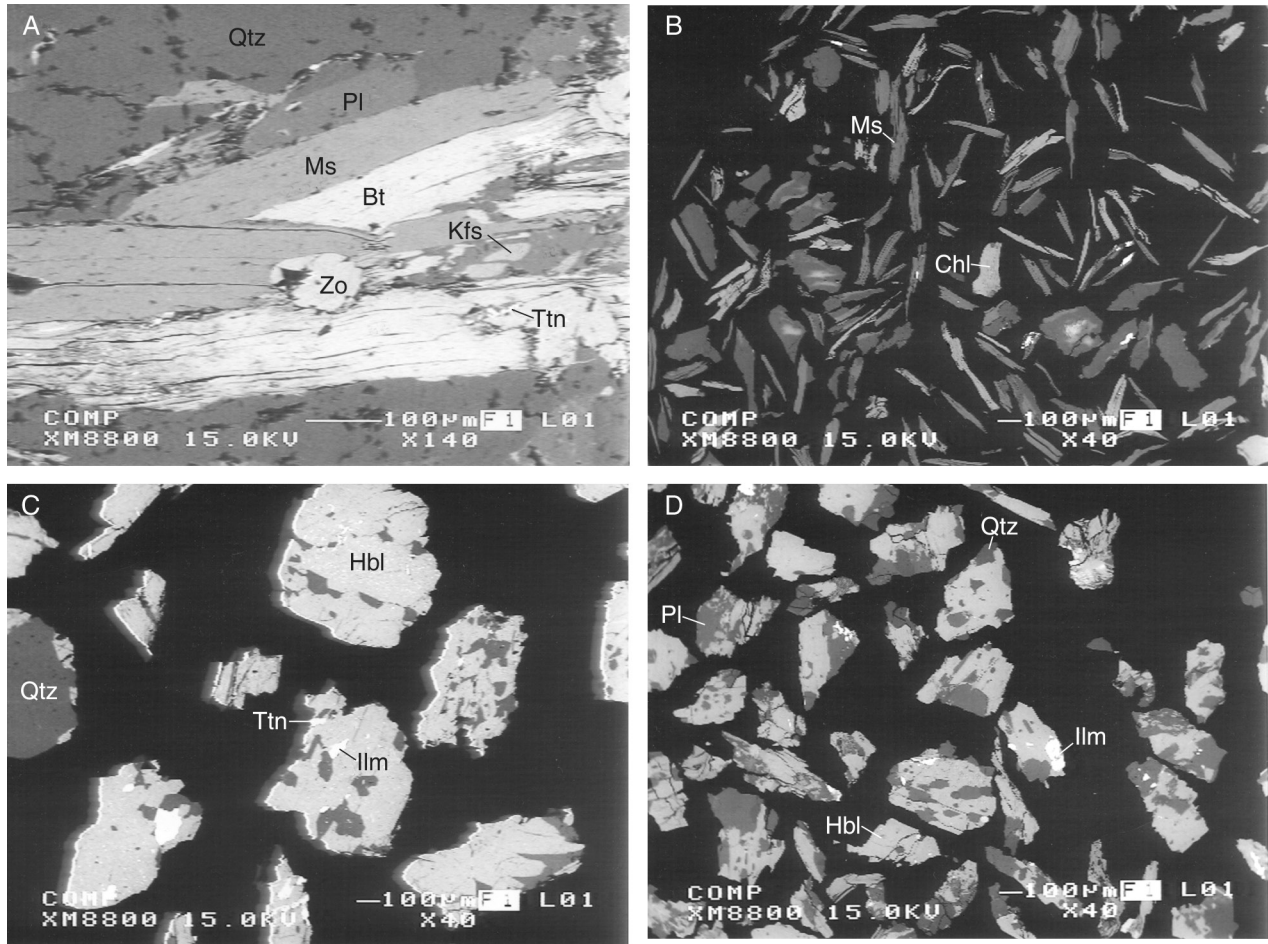


Fig. 5 (concluded).



**Fig. 6.** Backscattered electron images of selected minerals analyzed by  $^{40}\text{Ar}/^{39}\text{Ar}$  methods. (A) Ms and Bt grains in polished thin section of Qtz–Zo–Bt–Ms gneiss sample 11. (B) Ms separate from Grt–Chl–Wm–Qtz schist sample 22. (C) Hbl separate from Hbl–Ep–Qtz schist sample 23. (D) Hbl separate from Grt amphibolite sample 25.



ple 12) collected from within the fault zone. Although sample 12 shows minor alteration (sericite rims on Ky and minor, local chloritization of Bt, Hbl, and Grt, indicative of late-stage or subsequent hydration), Hbl from sample 12 gives a pseudoplateau age of  $165.6 \pm 0.8$  Ma (Fig. 5L). This age is an “intermediate” age between the well-established Early Jurassic (191–185) Ma metamorphic cooling ages of the Fortymile River assemblage and the Early Cretaceous (~120–108 Ma) metamorphic cooling ages of the Lake George assemblage. We interpret sample 12 to be part of the Lake George assemblage because it crops out ~200 m from amphibolite that has very distinctive alkaline, within-plate basalt chemistry that is typical of the Lake George assemblage but is not present in the Fortymile River assemblage (Dusel-Bacon and Cooper 1999). However, because the strain within the ductile fault zone is partitioned, coherent slices of either assemblage may be interleaved, and some rock types can occur in either assemblage, assignment to one or the other assemblage is equivocal.

#### Lake George assemblage metamorphic rocks

Amphibolite-facies schists and gneisses that can unequivocally be assigned to the Lake George assemblage all yield Early Cretaceous metamorphic cooling ages.  $^{40}\text{Ar}/^{39}\text{Ar}$  incremental step-heating experiments performed on Hbl sepa-

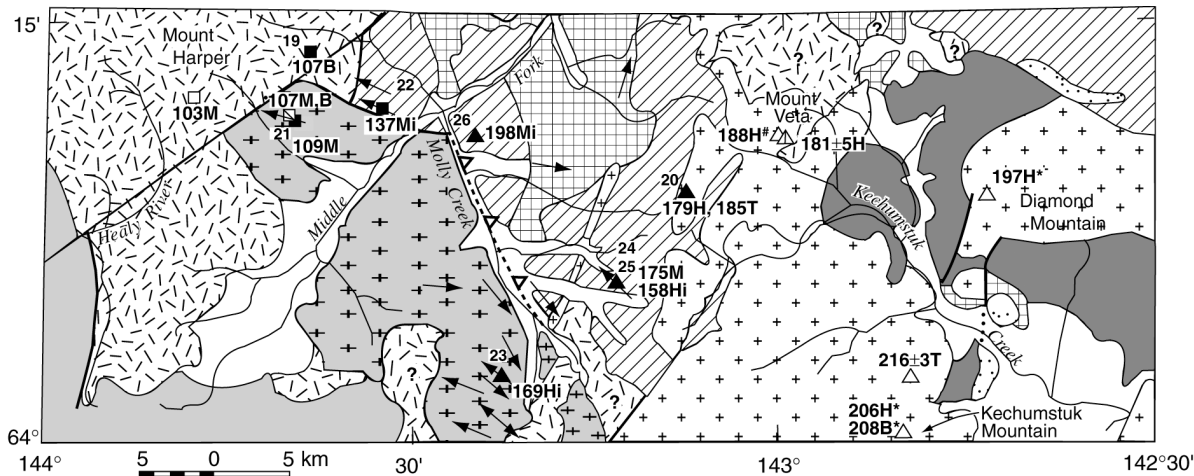
rated from amphibolite sample 13, which crops out within a large body of augen gneiss, yield slightly varying Early Cretaceous Ar release ages (Fig. 5M) that result in a very precise isochron age of  $119.2 \pm 0.8$  Ma and a pseudoplateau age of  $117.6 \pm 1.2$ . Four kilometres to the northeast, Hbl from a Grt–Qtz–Hbl schist (sample 14) gives a total fusion age of  $105.7 \pm 1.3$  Ma, and Ms from augen gneiss sample 15 yields a total fusion age of  $108.0 \pm 0.3$  Ma. Muscovite from the intensely sheared augen gneiss (shown in Fig. 4), within the fault zone, yields a plateau age of  $107.5 \pm 0.6$  Ma (Fig. 5N); Bt from the same sample (16) has a slightly hump-shaped spectrum (Fig. 5O), probably resulting from ductile deformation and minor alteration of the Bt (Appendix 1), and gives a plateau age of  $110.3 \pm 1.1$  Ma. Such hump-shaped spectra generally give plateau ages that are slightly too old and thus its true age may be about the same as that of the Ms. Similar Early Cretaceous total fusion ages were determined for micas from augen gneiss bodies to the east:  $110.6 \pm 0.7$  Ma and  $107.6 \pm 0.3$  Ma for Ms and Bt, respectively, from sample 17, and  $107.8 \pm 0.3$  Ma for Bt from sample 18.

#### Molly Creek area

##### Geologic setting

The Molly Creek area, located just west of Mount Veta in the southwestern Eagle quadrangle (Fig. 7), was chosen for

**Fig. 7.** Simplified geologic map of the Molly Creek area showing  $^{40}\text{Ar}/^{39}\text{Ar}$  ages and kinematic shear-sense indicators. Geology modified from Foster (1992); kinematic shear-sense indicators from Hansen and Dusel-Bacon (1998). Map unit patterns as on Fig. 2. Ages (in Ma) are rounded to nearest whole number; age uncertainties are given only for values  $> \pm 3$  Ma.



#### EXPLANATION

- ↖ Direction of displacement in structurally higher rocks; may be a composite from several adjacent stations.
- Cretaceous  $^{40}\text{Ar}/^{39}\text{Ar}$  age from this study; map i.d. number shown above age symbol.
- ▣ Cretaceous K–Ar age from Wilson et al. (1985).
- Cretaceous  $^{40}\text{Ar}/^{39}\text{Ar}$  age from Newberry et al. (1998b).
- ▲ Jurassic  $^{40}\text{Ar}/^{39}\text{Ar}$  age from this study; map i.d. number shown above age symbol.
- △ Jurassic K–Ar age from Wilson et al. (1985).
- △ Triassic or Jurassic age from other study.

Dated mineral: B, biotite; M, muscovite; H, hornblende; T, U–Pb titanite age (J.K. Mortensen, written commun.).

Unless otherwise specified, all  $^{40}\text{Ar}/^{39}\text{Ar}$  ages are plateau or pseudoplateau ages; i,  $^{40}\text{Ar}/^{39}\text{Ar}$  integrated age.

#  $^{40}\text{Ar}/^{39}\text{Ar}$  age from Cushing (1984).

\*  $^{40}\text{Ar}/^{39}\text{Ar}$  age from Newberry et al. (1998b).

thermochronometric analysis because it affords another view of Lake George assemblage augen gneiss, intruded by Cretaceous granitoids, in close proximity to Fortymile River assemblage rocks, which are intruded by Late Triassic and Early Jurassic granitoids. The nature of the covered contact between Lake George and Fortymile River assemblages, shown by Foster (1976) as occurring in the Molly Creek drainage, is conjectural. Foster et al. (1994) interpret the contact as a thrust fault in which Lake George assemblage rocks make up the upper plate. In contrast, we assume the interpretation of Dusel-Bacon et al. (1995) and Hansen and Dusel-Bacon (1998) to be correct, based on structural and thermochronologic data, in which the contact is a low-angle extensional fault that resulted from exhumation of lower plate Lake George assemblage rocks that were previously overthrust by the Fortymile River assemblage (see Hansen and Dusel-Bacon 1998 for discussion of the two models). The geologic setting and location of  $^{40}\text{Ar}/^{39}\text{Ar}$  samples analyzed in the Molly Creek area are shown in Fig. 7, along with the tectonic transport directions and a few isotopic ages for plutonic rocks determined in other studies. Kinematic analysis identified each of the three kinematic domains recognized to the east in the southeastern Eagle – Tanacross region (Hansen and Dusel-Bacon 1998), but the timing of the various deformations was uncertain.

#### Description of Ar release spectra

##### Plutonic rocks

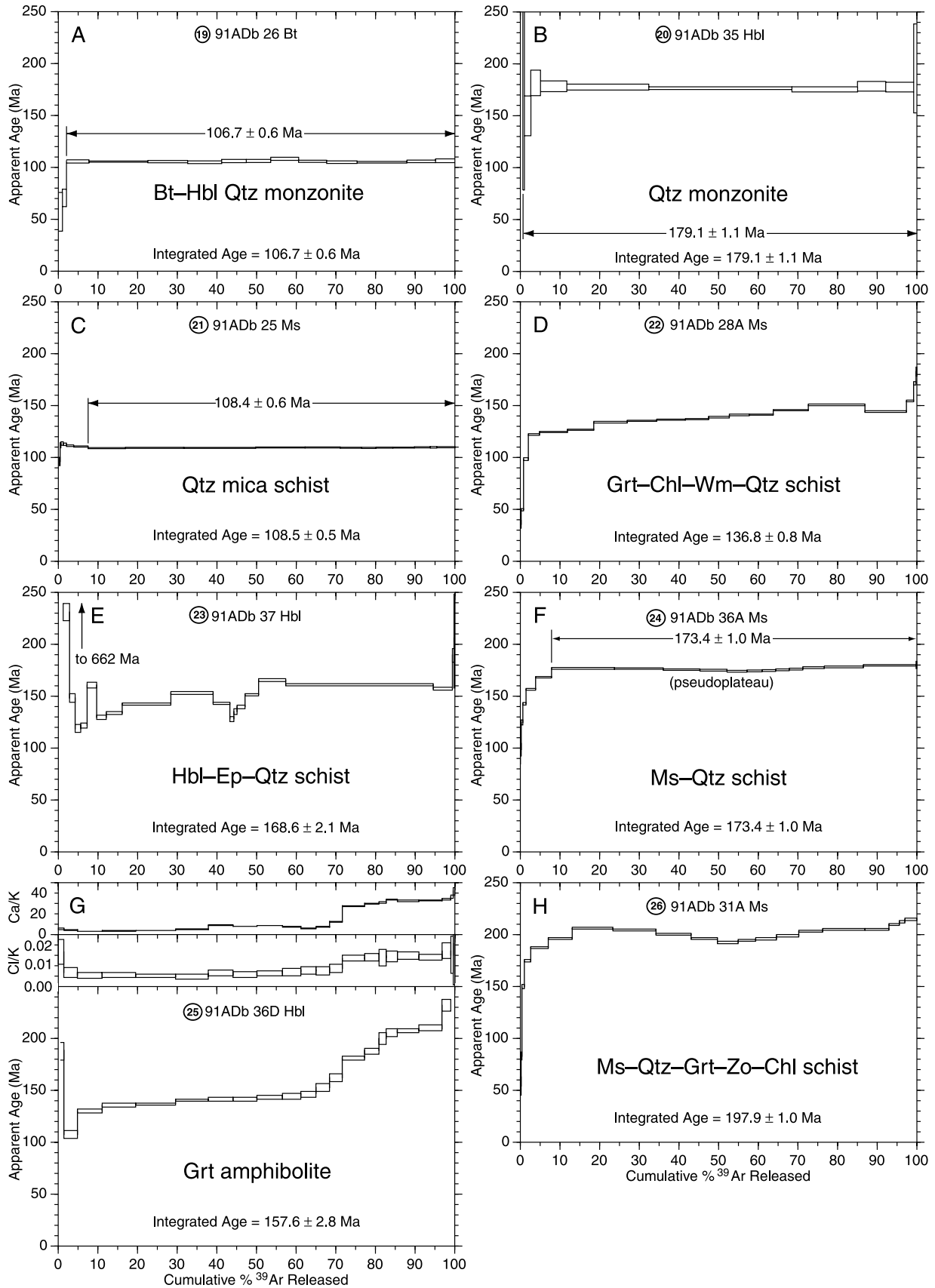
Biotite from fine-grained K-feldspar–Pl–Bt–Hbl monzonite (sample 19) from the eastern margin of the Mount Harper batholith gave a well-defined plateau age of  $106.7 \pm 0.6$  Ma (Fig. 8A). A slightly younger  $^{40}\text{Ar}/^{39}\text{Ar}$  plateau age of  $102.7 \pm 0.4$  Ma was obtained by Newberry et al. (1998b) on vein Ms from a porphyry W–Mo prospect within the Mount Harper batholith about 10 km southwest of our sample.

Hornblende from a coarse-grained Pl–K-feldspar–Hbl Qtz monzonite (sample 20) collected from the Mount Veta pluton yields a well-defined plateau age of  $179.1 \pm 1.1$  Ma (Fig. 8B). Titanite from this same sample gives a U–Pb age of  $185.4 \pm 1.4$  Ma (J.K. Mortensen, written communication, 2001). Conventional K–Ar analysis of Hbl from another location within this intrusion (Fig. 7) yielded an age of  $181 \pm 5$  Ma (Wilson et al. 1985) and a  $^{40}\text{Ar}/^{39}\text{Ar}$  plateau age of  $188 \pm 2$  Ma (Cushing 1984). We interpret the  $\sim 185$  Ttn age to be the closest approximation to the crystallization age of sample 20.

##### Metamorphic rocks

The Middle Fork of the Fortymile River forms a boundary between metamorphic rocks with Cretaceous cooling ages to the northwest and those with Jurassic cooling ages to the

**Fig. 8.** Ar release spectra for samples from the Molly Creek area. Box heights of each rectangle are  $\pm 1s$ .



southeast. Unfortunately, only two of our six metamorphic samples from the Molly Creek area yielded Ar plateaus; the other four gave complex spectra that reflect either superimposed deformational events or partial thermal resetting from nearby plutons. Sample 21, from an area of gneissic Qtz–Ms–Bt schist that crops out within a larger body of augen gneiss, yields a well-defined  $^{40}\text{Ar}/^{39}\text{Ar}$  Ms plateau age of  $108.4 \pm 0.6$  Ma (Fig. 8C). Conventional K–Ar ages on Bt and Ms from augen gneiss 0.5 km north of sample 21 are virtually identical at  $107.2 \pm 1.0$  and  $107.0 \pm 1.5$  Ma, respectively, (Wilson et al. 1985). Although sample 21 contains no petrographic evidence of static metamorphism, its proximity (~2 km) to the large Mount Harper batholith allows the possibility that its Ar may have been completely reset by the intrusion. However, our preferred interpretation is that the ages reflect cooling associated with ductile deformation.

Sample 22, a Chl–white mica quartzite–schist, was collected north of a northwest-striking high-angle fault that locally separates augen gneiss of the Lake George assemblage to the south from Fortymile River assemblage rocks to the north. Petrographic examination of sample 22 shows a polymetamorphic (retrograded) texture: Chl and white mica porphyroblasts occur both parallel to the foliation and at an angle to it, and Grt grains are skeletal. In outcrop, the sample is underlain by Chl–white mica schist with chloritized 4-mm Grt, and Chl books that form a lineation that may have formed during a later Chl-grade event. As might be expected, white mica from sample 22 gives a complex age spectrum with no identifiable plateau and monotonically rising age spectra with ages from about 120 to 155 Ma (Fig. 8D). The highest meaningful temperature step has an age of ~181 Ma. Microprobe examination of the white mica separate indicates that Chl, Qtz, and albite grains make up as much as ~10% of the mineral separate as either individual crystals or parts of the white mica grains (Fig. 6B). It is unlikely that these contaminants are the cause of the complex spectrum, and it is more likely that the disturbance of the Ar systematics are due to a mixed population of white micas and a partial resetting of original micas, most likely resulting from polyphase deformation and cooling. Proximity of the Mount Harper batholith allows the possibility that heat from that Cretaceous pluton also may have played a role in the disturbance of Ar systematics; however, Qtz grains in sample 22 show no evidence of annealing, and instead have undulose extinction and ragged subgrain boundaries.

All three of the metamorphic rock samples we collected southeast of the Middle Fork of the Fortymile River yield complex  $^{40}\text{Ar}/^{39}\text{Ar}$  age spectra and Jurassic integrated  $^{40}\text{Ar}/^{39}\text{Ar}$  ages (Table 2). Sample 23 is a Hbl schist that crops out within a 1-km-long ridge exposure of amphibolite and associated augen gneiss that occurs within a large augen gneiss body. The Hbl age spectrum for sample 23 is extremely irregular. Petrographic examination of sample 23 reveals that some of the larger Hbl porphyroblasts have cores containing finely crystalline to dusty Ilm. Microprobe examination of the Hbl separate (Fig. 6C) indicates relatively abundant inclusions of Qtz, and minor inclusions of Ilm, Ttn, and Chl. The Hbl spectrum may reflect a recoil redistribution of  $^{39}\text{Ar}$  and  $^{37}\text{Ar}$  into and out of the impurities.

Ms–Qtz schist (sample 24) and Grt amphibolite (sample 25) were collected from adjacent layers at the same locality

east of Molly Creek. The Ms–Qtz schist exhibits only a minor amount of sericitized and kaolinitized Pl and K-feldspar, but a sample of Bt–Grt gneiss from an adjacent layer shows intense retrograde alteration. Microprobe backscatter examination of the Ms showed it to be a virtually pure separate. Muscovite from the schist yields a pseudoplateau age of  $174.8 \pm 4.7$  Ma and has an age spectrum that is very slightly concave upward for all but the first six steps (Fig. 8F). This spectrum shape is like other muscovites that have cooled slowly or been partially reset (e.g., McDougall and Harrison 1999, p. 122).

Plagioclase in Grt amphibolite sample 25 is also highly kaolinitized, but the Hbl and Bt appear to be very fresh. Microprobe backscatter examination of the Hbl separate shows the grains to have a “leopard-like” appearance due to minute inclusions of sodic Pl, Qtz, Ilm, Di, Bt, Ms, Chl, and minor Ttn (Fig. 6D). Hornblende separated from the Grt amphibolite yields an age spectrum with older ages at the lowest and higher temperature steps (~186 Ma and ~230–300 Ma, respectively) and ages of ~140 Ma in the central part of the age spectrum that rise monotonically to ~220 Ma (Fig. 8G). Comparison of the Ca/K and Cl/K ratios for the Hbl (which indicate progressive changes in composition with heating) with the age spectrum (Fig. 8G) indicates a correlation of younger ages with lower Ca/K and Cl/K ratios. This correlation suggests that the younger ages of ~100–160 Ma that correspond with the lower compositional ratios (determined for ~2–72 cumulative % of the  $^{39}\text{Ar}$  released) may be due to contamination by included micas. Ages from about 180 to 208 Ma may be a more accurate indication of post-metamorphic cooling of Hbl through its blocking temperature.

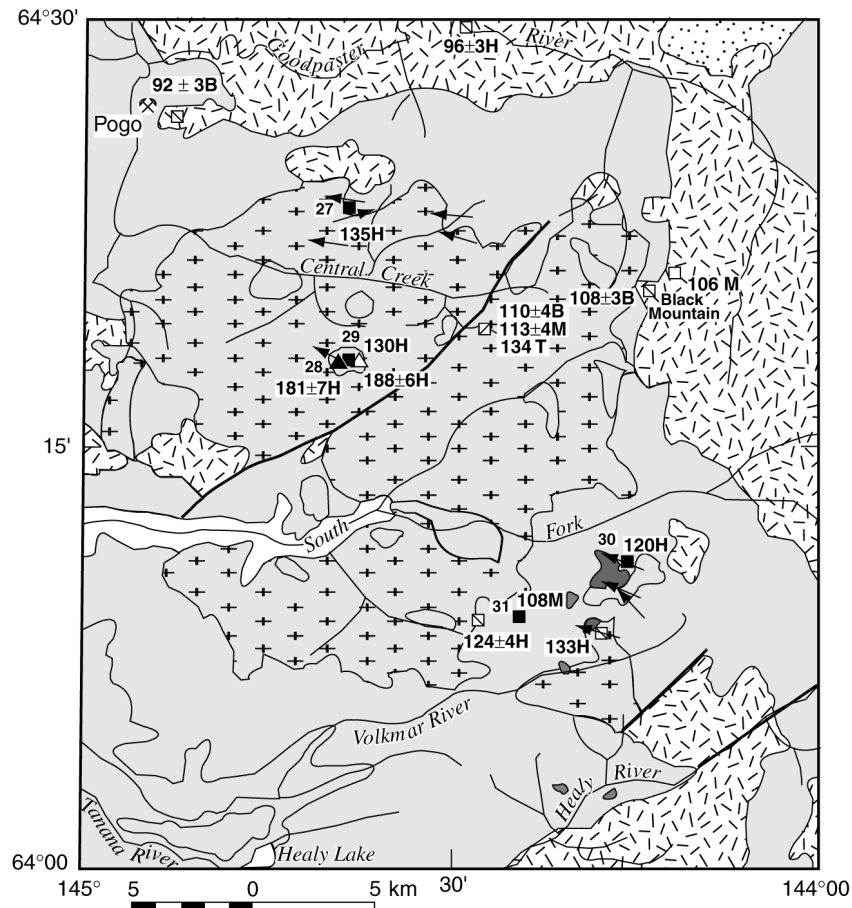
Muscovite from a Ms–Qtz–Grt–zoesite–Chl schist (sample 26) gives no plateau age, but the oldest  $^{40}\text{Ar}/^{39}\text{Ar}$  integrated and total fusion ages (~198 Ma; Table 2) for the metamorphic rocks sampled east of Molly Creek. All but the first six of the 20 incremental heating steps, form a concave upward pattern with central “trough” at about 190 Ma, rising to 213 Ma at the highest temperature step (Fig. 8H). The first six steps determined for sample 26 increase from about 54 to 195 Ma. Petrographic analysis of the sample indicates minor retrograde metamorphism and dynamothermal strain (Appendix 1). Backscatter electronic analysis of the Ms separate shows only rare Chl, Qtz, and Bt inclusions within a few Ms grains. We interpret the low-temperature steps to indicate a slight reset of Ar systematics, possibly by heating associated with nearby Jurassic and Early Cretaceous intrusions.

## Central Creek area

### Geologic setting

Lake George assemblage rocks of the southeastern part of the Big Delta  $1^\circ \times 3^\circ$  quadrangle are dominated by a ~700 km<sup>2</sup> batholith of mid-Paleozoic augen orthogneiss (Dusel-Bacon and Aleinikoff 1985), herein referred to as the Central Creek augen gneiss body (Fig. 9). Country rock to the augen gneiss body consists of amphibolite, Bt orthogneiss, Bt–Sil paragneiss, Qtz–mica schist, and quartzite. Several small foliated and regionally metamorphosed ultramafic masses are infolded with the amphibolite-facies gneiss and schist

**Fig. 9.** Simplified geologic map of the southeastern Big Delta quadrangle showing  $^{40}\text{Ar}/^{39}\text{Ar}$  ages and kinematic shear-sense indicators. Geology modified from Weber et al. (1978; kinematic shear-sense indicators modified from Hansen and Dusel-Bacon (1998). Map unit patterns as on Fig. 2 with the exception that units shown in dark grey consist of ultramafic rocks, many of which occur in small foliated masses infolded with amphibolite-facies gneiss and schist, which may have a different origin from those in the Seventymile terrane. Ages (in Ma) are rounded to nearest whole number; age uncertainties are given only for values  $> \pm 3$  Ma.



#### EXPLANATION

- ↖ Direction of displacement in structurally higher rocks; may be a composite from several adjacent stations.
  - Cretaceous  $^{40}\text{Ar}/^{39}\text{Ar}$  age from this study; map i.d. number shown above age symbol.
  - Cretaceous  $^{40}\text{Ar}/^{39}\text{Ar}$  age from Newberry et al. (1998b).
  - ⊠ Cretaceous K–Ar age from Wilson et al. (1985).
  - ⊞ Cretaceous K–Ar mica and U–Pb titanite ages from Aleinikoff et al. (1981).
  - ▲ Jurassic  $^{40}\text{Ar}/^{39}\text{Ar}$  age from this study; map i.d. number shown above age symbol.
  - △ Jurassic K–Ar Hornblende age from Wilson et al. (1985).
- Dated mineral: B, biotite; M, muscovite; H, hornblende; T, titanite. All  $^{40}\text{Ar}/^{39}\text{Ar}$  ages are plateau or pseudoplateau ages.

(Weber et al. 1978). A limited number of kinematic shear-sense indicators were determined in three areas in the vicinity of the Central Creek augen gneiss body (Fig. 9). Field and microstructural data from schist and orthogneiss indicate top-to-the-west-northwest shear at almost all localities (Hansen and Dusel-Bacon 1998). The locations of kinematic data shown on Fig. 9 supersede the locations for these data shown on Fig. 3 of Hansen and Dusel-Bacon (1998), as several samples were inadvertently misplotted in the previous publication.

We conducted incremental step-heating experiments on amphibolites from three different areas and Qtz-mica schist in one area that lie within or near the Central Creek augen gneiss body (Fig. 9). Previously published K–Ar ages for metamorphic rocks in the area include an important and anomalous Early Jurassic Hbl cooling age, in contrast with the typical Early Cretaceous K–Ar ages determined for the area (Wilson et al. 1985). Our study area lies just southeast of the recently discovered world-class lode-gold Pogo deposit (Smith et al. 1999; Fig. 9).

### Description of Ar release spectra

Amphibolite sample 27 is from a concordant layer, several tens of metres thick, within an area of quartzofeldspathic gneiss and Qtz–mica schist. These rocks occur as wall rock to the northern margin of the Central Creek augen gneiss body. Hornblende yields a pseudoplateau age of  $135.3 \pm 3.2$  Ma (Fig. 10A). Steps rising onto the pseudoplateau range widely in age, have large uncertainties, and show no consistent pattern. Backscattered electron examination of the Hbl separate show the grains to be homogeneous, with the exception of very minor Rt, Ilm, and Ttn inclusions observed in only a few grains.

Incremental heating experiments were performed on three samples from a small, 3.4-km<sup>2</sup> inlier of mafic schist and gneiss in the center of the Central Creek augen gneiss body (Fig. 9). Sample 28 was collected from an area of garnetiferous Hbl–Pl–Qtz gneiss, locally infolded with Zo–Hbl gneiss. In thin section, Grt forms irregular patches of granules that are probably remnants of former porphyroblasts, now partially replaced by Pl; margins of Rt grains have been altered to Ilm. Backscatter electron imaging of the Hbl separate shows it to be very homogeneous with only minor, local alteration of Chl in a few grains. Hornblende gives an Early Jurassic  $181.0 \pm 6.5$  Ma plateau age, but several steps within the incremental heating experiment give Early Cretaceous ages with large uncertainties (Fig. 10B). Hbl from mafic schist sample 29, collected ~150 m east of sample 28, gives complex a <sup>40</sup>Ar/<sup>39</sup>Ar spectrum with Cretaceous ages for all steps and a  $130.4 \pm 1.1$  Ma Hbl pseudoplateau age based on the two highest temperature fractions and 43% of gas release (Fig. 10C). Amphibolite collected ~500 m east of sample 28 yielded a Jurassic K–Ar age of  $188.0 \pm 5.6$  Ma (Wilson et al. 1985). Samples 28 and 29 are 19 km from the large (~22 km radius) Early Cretaceous batholith that makes up Black Mountain on its western margin (Fig. 9) and Mount Harper on its eastern margin. Proximity to the batholith allows the possibility that Ar in Hbl samples 28 and 29 may have experienced partial thermal resetting from the batholith, but the Qtz petrofabric in the samples (undulose extinction and ragged subgrain boundaries) records strain, not static recrystallization.

Amphibolite (sample 30) crops out at the northern margin of a serpentinized ultramafic body, the largest of the small foliated and regionally metamorphosed ultramafic masses infolded with the amphibolite-facies rocks in the area (Fig. 9). The amphibolite overlies a small augen gneiss body and directly underlies a several m-thick layer of Grt amphibolite that occurs at the base of the ultramafic body. Electron microprobe examination of the Hbl separate from sample 30 indicates minor Qtz and Ttn inclusions within some amphibole crystals as well as minute streaks of Chl or actinolite (2–3 microns long) locally within a few grains. The Hbl gives a plateau age of  $120.4 \pm 0.7$  Ma; younger ages were determined for lower temperature steps (Fig. 10D). Because there is no consistent relationship between age and Ca/K ratio at low temperatures, it is unlikely that the ~100–110 Ma ages reflect contaminant phases within the Hbl. It is possible that the lower temperature steps reflect partial thermal resetting by the Early Cretaceous batholith to the east, but there is no petrographic evidence for static heating.

Sample 31, a garnetiferous mica schist from wall rock to the southeastern margin of the Central Creek augen gneiss body occurs at the only locality in the southeastern Big Delta quadrangle at which Ky was identified during reconnaissance mapping. Muscovite from sample 31 gives a relatively undisturbed age spectrum with a plateau age of  $108.3 \pm 0.6$  Ma (Fig. 10E), similar to Ms ages elsewhere in the Lake George assemblage. The proximity of sample 31 (10 km) to the ~12.5 km-radius undated Early Cretaceous(?) pluton of the Healy River allows the possibility of some thermal resetting of the sample by the pluton. The observation that the Bt in sample 31 is fresh and reddish brown in some folia but is Fe-stained, full of Rt needles, or greenish in many other folia and that the Pl is moderately Fe-stained along cleavages (Appendix 1), indicates retrograde effects from hydrothermal fluids. These fluids could have been pluton-derived, but Qtz petrofabric in the sample (undulose extinction and ragged grain and subgrain boundaries) indicate crystallization under dynamothermal conditions, suggesting that retrograding fluids accompanied deformation rather than static pluton-related recrystallization. We conclude that the well-developed plateau for the Ms spectrum and the occurrence of unaltered porphyroblasts of Grt, St, and Ky and fresh Ms observed in thin section indicate that these higher *T* phases were unaffected by lower *T* fluids that retrograded the Bt and, therefore, that the Ms age does, in fact, represent cooling from metamorphic crystallization.

### Eastern flank of Salcha River gneiss dome

<sup>40</sup>Ar/<sup>39</sup>Ar analysis was performed on three samples of Lake George assemblage amphibolite-facies schist (collected by W.J. Nokleberg and colleagues) from the eastern margin of the Salcha River gneiss dome (Fig. 2). Sample 32 is a Hbl–Pl–Bt schist, interlayered with Qtz–mica schist, in which coarse Hbl crystals to 2 cm long are randomly oriented within the foliation plane. Zones of mottled, granitic-appearing foliated rocks in the outcrop area suggest incipient melting and recrystallization in quartzofeldspathic schists (G. Plafker, unpublished data, 1987), similar to that documented in other parts of the gneiss dome (Dusel-Bacon and Foster 1983). Hornblende and Bt from sample 32 yield well-defined plateau ages of  $113.6 \pm 2.8$  and  $109.3 \pm 0.6$  Ma, respectively, (Figs. 10F, 10G). Hornblende from mafic schist (sample 33) gives a complex spectrum with a mixture of Late Triassic, Jurassic, and Early Cretaceous <sup>40</sup>Ar/<sup>39</sup>Ar apparent ages (Fig. 10H). The northernmost sample, a Qtz–Ms schist (sample 34), gives a Ms <sup>40</sup>Ar/<sup>39</sup>Ar plateau age of  $109.6 \pm 0.6$  Ma (Fig. 10I), indistinguishable from the Bt age of sample 32.

## Discussion

Integration of our <sup>40</sup>Ar/<sup>39</sup>Ar data with <sup>40</sup>Ar/<sup>39</sup>Ar and U–Pb ages, shear-sense indicators (Figs. 3, 7, 9), and metamorphic *P–T* determinations (Dusel-Bacon et al. 1995) confirms and refines the complex interaction of plutonism, metamorphism, and deformation in the central and eastern Yukon–Tanana Upland.

**Fig. 10.** Ar release spectra for samples from the southeastern Big Delta quadrangle. Box heights of each rectangle are  $\pm 1\sigma$ .

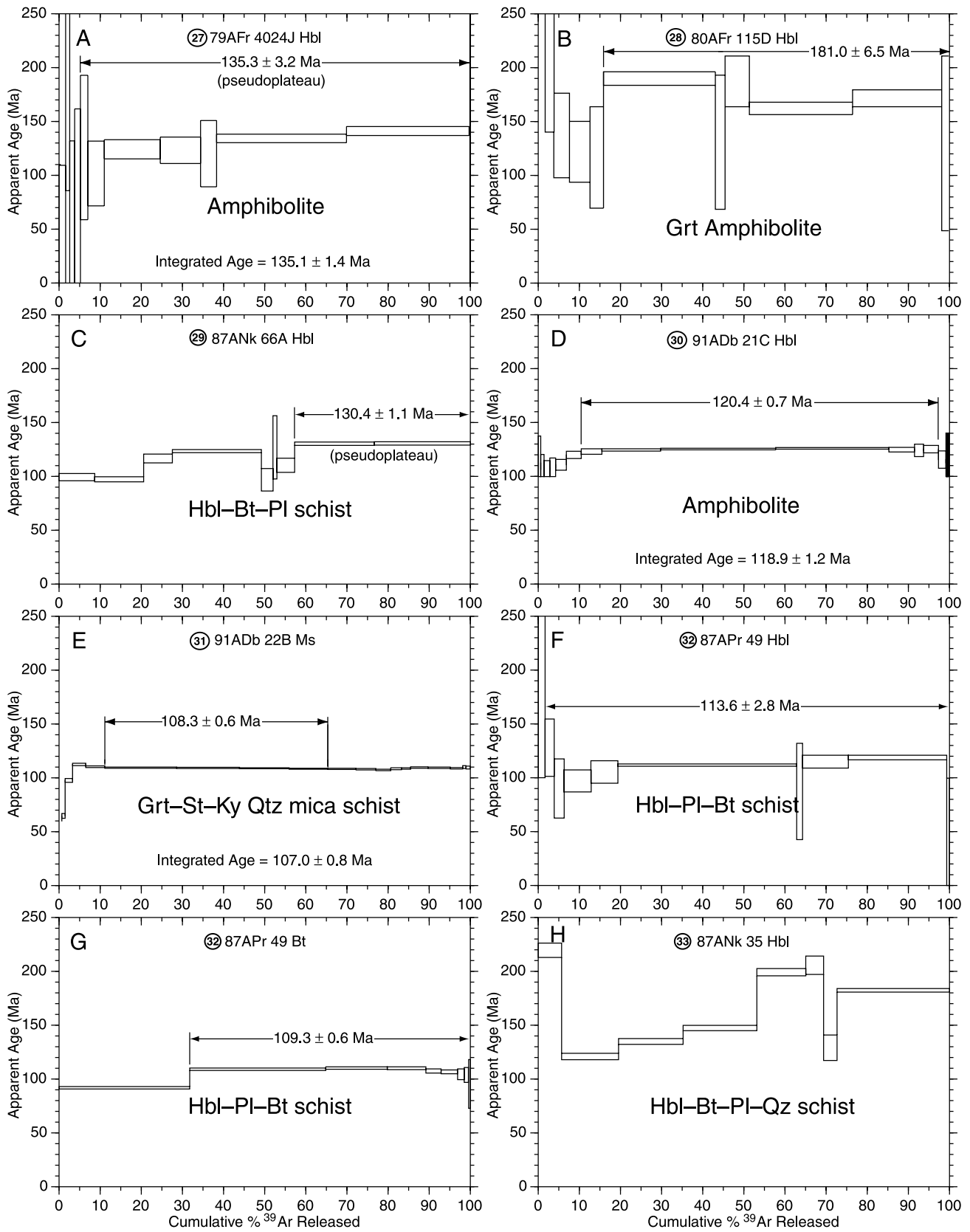
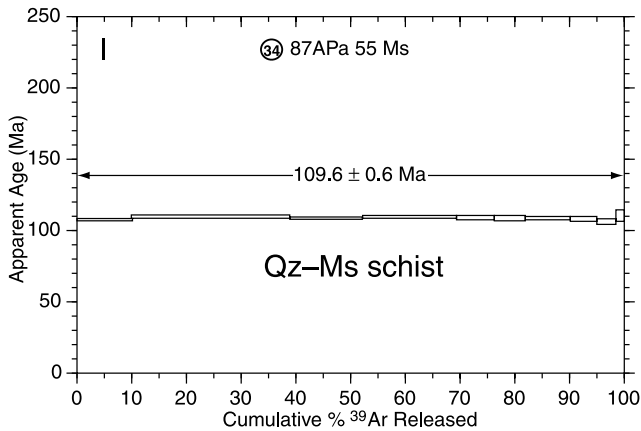


Fig. 10 (concluded).



### Late Triassic plutonism and pre-Late Triassic (> ~215 Ma) metamorphism

Hansen et al. (1991) identified a top-to-the-north-northeast tectonic transport direction in penetratively deformed and metamorphosed L-S tectonites in the northern, and structurally high, part of the Fortymile River assemblage in the eastern Eagle quadrangle (Fig. 3). Hansen and Dusel-Bacon (1998) proposed that northeast-vergent deformation corresponded with an early phase of metamorphism that preceded intrusion of the Late Triassic Taylor Mountain batholith. Intermediate- to high- $P$  and  $T$  metamorphism (ca. 8–12 kbar and ca. 550–700°C) accompanied the north-northeast-vergent, orogen-normal deformation (Dusel-Bacon and Hansen 1992; Dusel-Bacon et al. 1995).

The Taylor Mountain batholith, which contains foliated xenoliths, gives a concordant U–Pb age on Ttn of 212 Ma (Aleinikoff et al. 1981) and Hbl and Bt  $^{40}\text{Ar}/^{39}\text{Ar}$  plateau ages of  $209 \pm 3$  Ma and  $204 \pm 9$  Ma, respectively, (Cushing 1984). Similar  $^{40}\text{Ar}/^{39}\text{Ar}$  plateau ages of  $210 \pm 2$  Ma on Hbl and  $211 \pm 2$  Ma on Bt from a sample of granodiorite just north of the Mosquito Fork (Fig. 3; Szumigala et al. 2000a) suggest that the granodiorite is an apophysis of the Taylor Mountain batholith.

New isotopic ages for plutonic rocks that crosscut the metamorphic fabric in the Molly Creek area (Fig. 7) suggest that the pre-Late Triassic (> ~215 Ma) metamorphic event extended as far west as Molly Creek. Titanite from weakly foliated granodiorite collected 4 km north of Kechumstuk Mountain gives a concordant Ttn U–Pb age of  $215.7 \pm 3.1$  Ma (J.K. Mortensen, written communication, 2001) and granodiorite from Kechumstuk Mountain itself yields undisturbed  $^{40}\text{Ar}/^{39}\text{Ar}$  plateau ages of  $205.6 \pm 1.0$  Ma and  $207.8 \pm 1.2$  Ma for Hbl and Bt, respectively, (Fig. 5; Newberry et al. 1998b). Because Ttn has a higher blocking temperature (~700°C; Zhang and Schärer 1996; Pidgeon et al. 1996) than Hbl (~450°C) or Bt (~300°C), we interpret the Ttn U–Pb age to be closer to the true crystallization age of the Kechumstuk pluton, assuming that it is, indeed, a single intrusive body. Although Ms from sample 26, located east of Molly Creek, displays a disturbed  $^{40}\text{Ar}/^{39}\text{Ar}$  spectrum, the predominance of Late Triassic and earliest Jurassic step-heating ages (Fig. 8H; Table D2) is consistent with a partial resetting of the pre-Late Triassic metamorphic event by sub-

sequent Early Jurassic plutonism and metamorphism, and possibly also by mid-Cretaceous extension and posttectonic plutonism, as suggested by the petrographic evidence of minor retrograde metamorphism.

A minimum metamorphic age for the greenschist-facies rocks of the Nisutlin assemblage is harder to establish. The only indirect age constraint is a Late Triassic  $^{40}\text{Ar}/^{39}\text{Ar}$  age of  $214.4 \pm 0.6$  Ma (Newberry et al. 1998b) for Ms from a greisen vein that crosscuts the slightly foliated Happy granite intrusion that crops out north of our study area (just west of the northwest corner of the outline for Fig. 3, shown on Fig. 2).

This same minimum metamorphic age is also indicated by the Late Triassic age (Poulton et al. 1999) of sediments, which are only weakly deformed, and are imbricated by thrust faults that interleave the low-grade sediments, greenstone, and serpentinite of the Seventymile terrane, with the penetratively deformed Nasina assemblage, near Clinton Creek, just east of the Alaska–Yukon border (Mortensen 1988; 1990).

Structural investigations across the north-vergent thrust zone that juxtaposes the Fortymile River and Nisutlin assemblages (Fig. 3) indicate that, although both assemblages display tight to isoclinal folds with gently plunging fold axes, fold axes in the greenschist-facies Nisutlin schists are east-southeast trending, whereas those in the amphibolite-facies Fortymile River assemblage schists and gneisses are north-northeast trending (Cushing 1984; Foster et al. 1985). Despite the difference in the orientation of fold axes in these two assemblages, there is a general north-northeast concordance in the trend of moderately developed elongation lineations (Hansen et al. 1991; Hansen and Dusel-Bacon 1998) (Fig. 3). The generally consistent trend of elongation lineations within the Fortymile River and Nisutlin assemblages suggests that they share, at least in part, a common structural history. The difference in the orientation of the fold axes preserved within these two packages may reflect the crustal level at which each of these assemblages was deformed: fold axes and elongation lineation are parallel in the highly strained amphibolite-facies rocks of Fortymile River assemblage, whereas fold axes are oriented normal to transport direction at shallow crustal levels in the greenschist-facies rocks of the Nisutlin assemblage (Hansen et al. 1991). Thus, structural observations, together with identical minimum metamorphic age constraints for the Fortymile River and Nisutlin assemblages, are consistent with synchronous pre-Late Triassic initial metamorphism of both assemblages.

A Middle Permian maximum age for the pre-Late Triassic metamorphic episode is provided by the U–Pb zircon protolith ages of the youngest dynamothermally metamorphosed rocks:  $262 \pm 2$  Ma for the Sulphur Creek orthogneiss and related felsic metavolcanic rocks (Klondike Schist; included as part of the Nisutlin assemblage; Fig. 1) in west-central Yukon (Mortensen 1990), and  $257 \pm 1$  Ma for metarhyolite within Nasina assemblage rocks just west of the Alaska–Yukon border (Dusel-Bacon et al. 1998).

### Early Jurassic contractional deformation, metamorphism, and plutonism in the southeastern Eagle quadrangle

The Early Jurassic plutonic rocks, although locally weakly foliated, generally have equigranular textures, in contrast

with their penetratively deformed and metamorphosed wall rocks. This observation suggests that the plutons postdate both the first (northeast-vergent) deformation and the second (northwest-vergent), and more widespread, deformation recorded in Fortymile River assemblage tectonites. Contacts between these plutons and the adjacent metamorphic wall rocks are generally not exposed and, in many places, steep faults have been mapped between exposures of weakly foliated plutonic rocks and penetratively deformed metamorphic rocks (Szumigala et al. 2000b; J.M. Proffett, unpublished report for Kennecott Exploration 1999), precluding structural comparisons between wall rock and pluton fabrics. Detailed mapping within and adjacent to the Napoleon Creek pluton by J. M. Proffett found that, at one locality within the western part of the pluton, the main metamorphic layering and folds that fold this layering appear to be intruded by dikes of Hbl monzonite, thus indicating that both of these deformations are older than the pluton.

$^{40}\text{Ar}/^{39}\text{Ar}$  metamorphic cooling ages indicate the time of cooling through the blocking temperature for the dated mineral, but these ages do not indicate the time at which fabric formation was initiated. It is possible that initiation of the northwest-vergent fabric predated not only the Early Jurassic intrusions but also the Late Triassic intrusions, such as the Taylor Mountain batholith. The predominance of 188–186 Ma  $^{40}\text{Ar}/^{39}\text{Ar}$  Hbl, Ms, and Bt ages in both the Early Jurassic plutons (Mount Warbelow, Chicken, Napoleon Creek, and Pig plutons) and the Fortymile River assemblage metamorphic rocks could either indicate that (1) the metamorphic ages were reset by the plutons, or that, (2) the entire region was at mid-crustal depths prior to this time and was rapidly cooled at ~188–186 Ma. As stated earlier, in spite of the proximity of some of the metamorphic samples in the southeastern Eagle quadrangle to plutons of known or suspected Early Jurassic age, there is little textural evidence (except in sample 5) to suggest that their  $^{40}\text{Ar}/^{39}\text{Ar}$  ages may have been partially or totally reset by the nearby plutons. Moreover, 186–188 Ma metamorphic cooling ages also have been determined for samples more distant to these plutons, and, most importantly, have been determined for two samples located within thrust zones and 10–15 km from any known plutons (our sample 4 and a 187 ± 2 Ma  $^{40}\text{Ar}/^{39}\text{Ar}$  plateau age for Bt (Cushing 1984) from within a north-vergent thrust zone exposed along the Fortymile River (Fig. 3), presumably correlative with the thrust system that placed the Fortymile River assemblage onto the Nasina assemblage (Foster et al. 1985)).

Foster et al. (1985) state that the overall movement of the amphibolite-facies rocks (Fortymile River assemblage) is believed to be northwestward and that thrusting appears to have taken place both at relatively shallow depths (as indicated by formation of breccias and brittle fault zones) and at deeper levels where deformation is ductile. Subsequent kinematic and  $^{40}\text{Ar}/^{39}\text{Ar}$  studies of the Fortymile River assemblage tectonites south of the Fortymile River (Hansen et al. 1991; Hansen Dusel-Bacon 1998) showed that top-to-the-northwest shear was widespread in the central and southern Fortymile River assemblage and that exhumation and rapid cooling of the northwest-vergent tectonites in that area from ~450°C (blocking temperature of Hbl) through ~300°C (blocking temperature of Bt) occurred at ~188–186 Ma

(Fig. 3). Metamorphic cooling ages of 186 Ma for three of our Fortymile River assemblage samples (nos. 5, 7, 9) are near samples that give a top-to-the-northwest sense of shear (Fig. 3). We, therefore, favor alternative 2 and conclude that rapid cooling of both the plutons and their mid-crustal wall rocks accompanied northwest-vergent thrusting.

We propose that Early Jurassic (~188–186 Ma) plutonism in the Fortymile River area (Fig. 3) was late- to posttectonic with respect to northwest-vergent contractional deformation and the final stages of amphibolite-facies metamorphism. Permissive evidence for a late-tectonic relationship is the overlap of the  $^{40}\text{Ar}/^{39}\text{Ar}$  Hbl and mica metamorphic cooling ages from the Fortymile River assemblage tectonites containing northwest-vergent fabrics with the Hbl  $^{40}\text{Ar}/^{39}\text{Ar}$  plateau ages from the Chicken, Napoleon Creek, and Pig plutons. Zircon and Ttn separated from Napoleon Creek pluton sample yield concordant U–Pb ages of  $188.4 \pm 1.2$  Ma and  $188.0 \pm 1.7$  Ma, respectively, (J.K. Mortensen, written communication, 2001) and Hbl from the same sample gives a  $^{40}\text{Ar}/^{39}\text{Ar}$  plateau age of a  $186.6 \pm 1.0$  Ma (Fig. 3), indicating a potentially rapid progression of igneous crystallization and cooling from ~700 to ~450°C. The local development of weakly to moderately well-developed fabrics within parts of the 186-Ma plutons (Szumigala et al. 2000b) is also consistent with a late- to posttectonic origin. Regional uplift related to thrusting also would explain the coincidence of ~188–186 Ma  $^{40}\text{Ar}/^{39}\text{Ar}$  cooling ages in plutonic and metamorphic rocks throughout much of the southeastern Eagle quadrangle (Fig. 3).

We interpret the ~210–195 Ma  $^{40}\text{Ar}/^{39}\text{Ar}$  metamorphic cooling ages in the southeastern Eagle quadrangle to be Late Triassic or older metamorphic ages that have been partially reset by the ~186 Ma plutono-metamorphic contractional episode. All of the  $^{40}\text{Ar}/^{39}\text{Ar}$  metamorphic Hbl plateau ages reported by Cushing (1984) for amphibolites ( $213 \pm 2$  Ma,  $204 \pm 4$  Ma, and  $194 \pm 2$  Ma; Fig. 3) are from disturbed age spectra indicative of a complex cooling history. Our  $202.4 \pm 1.6$  Ma total fusion mean age for Grt amphibolite sample 10, is probably also an average of the ages for several different phases of deformation and metamorphism.

### Early Jurassic metamorphism overprinted by Early Cretaceous metamorphism

#### *Northeastern Tanacross quadrangle*

Dusel-Bacon et al. (1995) and Hansen and Dusel-Bacon (1998) showed a continuity of mineral elongation orientation, top-to-the-northwest vergence, and similar intermediate- to high-*P* amphibolite-facies metamorphic conditions on either side of the ductile fault zone between the upper plate Fortymile River assemblage and lower plate Lake George assemblage (Fig. 3). These kinematic and metamorphic similarities led the above authors to propose that the episode of northwest-directed shear and accompanying metamorphism affected both assemblages as they were being juxtaposed during the Early Jurassic shortening episode. A likely explanation for the fact that the 166 Ma metamorphic cooling age of sample 12, from the western part of the fault zone, is 20 million years younger than the 186 Ma rapid cooling ages of mineral pairs in the southern Fortymile River assemblage is the structurally lower position of this sample relative to the

rocks with 186 Ma ages to the north and, hence, delayed cooling following Early Jurassic tectonism (Hansen and Dusel-Bacon 1998).

All other  $^{40}\text{Ar}/^{39}\text{Ar}$  metamorphic cooling ages from the Lake George assemblage, south of the fault zone, are exclusively mid-Cretaceous (Fig. 3). With the exception of sample 18 and a sample at the western edge of the area shown in Fig. 3 that was dated by Hansen et al. (1991), all other  $^{40}\text{Ar}/^{39}\text{Ar}$  metamorphic samples are located too far away from plutons (at a distance  $\gg$  than the radius of the pluton) to have a thermal resetting of the Ar systematics be a plausible explanation for their Cretaceous ages. Sample 18 is 3.5 km from Crag Mountain pluton, estimated to have a radius of 4.2 km, from which a  $107.5 \pm 1$  Ma U–Pb monazite age was determined from its eastern margin in the Yukon (J.K. Mortensen, oral communication, 2001), and the westernmost sample, dated by Hansen et al. (1991) is 12.5 km from an undated granitoid batholith that has a radius of  $\sim 17.5$  km (Fig. 2). Neither of these samples shows any textural evidence of static thermal metamorphism but, instead, has the same ductile deformational fabrics present in other rocks of the Lake George assemblage that are more distant from plutons.

Top-to-the-northwest shear dominates in the northern, structurally higher part of the section, and younger, top-to-the-southeast shear dominates in the southern, structurally lower part of the section. Some rocks within the fault zone exhibit both fabrics. We interpret cooling related to top-to-the-southeast shear to be constrained by Hbl, Ms, and Bt cooling ages of  $\sim 119$ , 109, and 109 Ma, respectively, (Fig. 3). Although kinematic indicators were not present our sample 13, which yielded a 119 Ma Hbl isochron age, nor in the granitic gneiss sample, 1.7 kms away, which gave the 109 Ma Ms and Bt plateau ages (Hansen et al. 1991), southeast-directed shear dominates in both areas (Fig. 3). Thus, we infer that top-to-the-southeast tectonites in those areas cooled from  $\sim 450$  to  $300^\circ\text{C}$  in 10 million years. Quartz grains in many top-to-the-southeast tectonites show microscopic textures indicative of low-temperature plasticity, such as strong undulose extinction, ragged grain boundaries, and subgrain growth. The lack of annealed textures, combined with the relatively fast cooling rate, indicates that ductile shear accompanied metamorphic cooling (Hansen and Dusel-Bacon 1998).

A 135-Ma  $^{206}\text{Pb}/^{238}\text{U}$  age was determined for Ttn from ductilely deformed augen gneiss sample 18 (Dusel-Bacon and Aleinikoff 1996), for which southeast-vergent deformation was measured. Unfortunately, the geologic significance of this age is unclear. Recent studies show that the closure temperature for U–Pb ages in Ttn are about  $700^\circ\text{C}$  (e.g., Pidgeon et al. 1996; Zhang and Shärer 1996), at or above the upper limit of the amphibolite facies. Thus, in metamorphic rocks that crystallized below this temperature, U–Pb ages of Ttn are likely to represent the time of metamorphic growth or crystallization, rather than cooling through the closure temperature (Frost et al. 2000). Although a peak metamorphic  $T$  was not calculated for sample 18, a peak metamorphic  $T$  of  $640$ – $700^\circ\text{C}$  was determined for pelitic schist collected  $\sim 3$  km from sample 18 (Dusel-Bacon et al. 1995). Because the possibility exists that sample 18 may have approached or surpassed the  $\sim 700^\circ\text{C}$  closure temperature for

Ttn, its 135 Ma U–Pb age could date either metamorphic crystallization or cooling through  $\sim 700^\circ\text{C}$ . In addition, because Ttn is a relatively reactive mineral whose abundance and composition reflect changes in  $P$ ,  $T$ , and composition of the metamorphic fluid, a rock that experienced a complicated thermal history may contain multiple generations of Ttn. U–Pb data from Ttn containing multiple age components may be mixtures of ages and, as such, may be geologically meaningless. We tentatively interpret the  $\sim 135$  Ma age for Ttn from augen gneiss sample 18 that was previously dated by conventional U–Pb geochronology (Dusel-Bacon and Aleinikoff 1996; Fig. 3) as a crystallization age for metamorphism and deformation associated with top-to-the-southeast deformation and exhumation of the lower plate Lake George assemblage. However, we recognize that more detailed backscatter imaging of Ttn zoning and in situ dating of individual grains might yield more reliable results.

At the western edge of our study area, a peraluminous augen orthogneiss with top-to-the-northwest fabric yielded Ms and Bt cooling ages of 110 and 111 Ma, respectively, (Fig. 3; Hansen et al. 1991). Hansen and Dusel-Bacon (1998) state that although the sample contains the earlier formed top-to-the-northwest shear fabric, it probably cooled through the mica blocking temperatures during tectonic denudation related to top-to-the-southeast shear. We propose the same explanation for the 108 Ma Ms metamorphic cooling age of sample 16 that contains both the northwest- and southeast-vergent fabrics. According to this interpretation, the preserved top-to-the-northwest fabrics formed at temperatures above the  $^{40}\text{Ar}/^{39}\text{Ar}$  blocking temperatures for Ms and Bt, and the samples remained buried until the top-to-the-southeast extensional event.

The 177 Ma Ms plateau and 124 Ma Bt pseudoplateau  $^{40}\text{Ar}/^{39}\text{Ar}$  ages from sample 11, a gneiss located within the eastern part of the fault zone, elucidates the superposition of tectonic events within the region — (1) Early Jurassic crustal thickening and metamorphism during northwest-vergent contraction; (2) continued tectonic burial until mid-Cretaceous time; and (3) unroofing of lower plate rocks during mid-Cretaceous southeast-vergent extension — in a single sample. Top-to-the-southeast deformation was measured at the locality from which the sample was collected, but top-to-the-northwest deformation also occurs within a couple of kilometres to the north. The structurally low position of sample 11, relative to structurally overlying Fortymile River assemblage tectonites to the north that yield  $\sim 186$  Ma metamorphic cooling ages, is consistent with the later time at which this deeper sample rose through the Ms blocking temperature, analogous with our interpretation of the 166 Ma age for sample 12. The textural evidence (Fig. 6A), suggesting that both minerals formed at the same time, implies that both phases were formed during the Early Jurassic event and the sample cooled through  $\sim 375^\circ\text{C}$  at  $\sim 177$  Ma but remained above  $\sim 300^\circ\text{C}$  prior to  $\sim 124$  Ma; consistent with the Early Jurassic contraction – mid-Cretaceous extension model.

#### Molly Creek area

Most metamorphic samples from the Molly Creek area yield complex  $^{40}\text{Ar}/^{39}\text{Ar}$  age spectra and have petrographic evidence of retrograde metamorphism. In addition, some of these samples are close enough to Early Jurassic or Creta-

ceous plutons to have experienced a partial thermal resetting by the plutons, although this is not evident in the textures of the rocks. For this reason, the metamorphic and deformational history in the area is difficult to decipher, but a polyphase dynamothermal history, comparable to that proposed for the eastern Eagle – Tanacross area, is consistent with many of our observations. At the location from which sample 22 was collected, northeast- and northwest-trending elongation lineations are preserved in different parallel foliations. Quartz petrofabrics from sample 22, while non-unique in origin, can be explained as a result of consecutive and coplanar, but perpendicular, shear events (Hansen and Dusel-Bacon 1998), consistent with the northeast- and northwest-trending elongation lineations in the outcrop. A single, northwest-vergent tectonic transport direction was measured in Fortymile River assemblage rocks at the locality from which samples 24 and 25 were collected (Fig. 7), but a polyphase metamorphic and deformational history is indicated by the highly complex age spectra determined for both samples, the intense retrograde alteration of a Bt–Grt gneiss from an adjacent layer in the outcrop, and abundant included phases in the Hbl separate (Fig. 6D). Our assumption that the  $^{40}\text{Ar}/^{39}\text{Ar}$  incremental step heating ages from ~180 Ma to 208 Ma for sample 25 give a general age range for the cooling of metamorphic Hbl through 450°C is consistent with the timing for top-to-the-northwest contractional deformation and metamorphism in the eastern Eagle quadrangle. The ~185 Ma crystallization age we infer for the nearby Mount Veta pluton indicates that Early Jurassic plutonism in this area, as in the southeastern Eagle quadrangle, may have been latest to post-kinematic with northwest-vergent deformation and metamorphism.

West of Molly Creek, S-C fabrics in peraluminous augen gneiss of the Lake George assemblage record both top-to-the-northwest and top-to-the-southeast ductile shear (Hansen and Dusel-Bacon 1998). Top-to-the-southeast shear occurred along more localized, discrete shear zones relative to the earlier, more penetratively developed top-to-the-northwest fabrics. Top-to-the-southeast tectonites typically display transitional ductile–brittle character. Sample 23, a Hbl schist, was collected from an area in which both fabrics have been measured at different outcrops and, at one locality (shown on Fig. 7 by a two-headed arrow), top-to-the-northwest S-C fabrics occur in peraluminous orthogneiss within both upper and lower plate positions with respect to a gently northeast-dipping top-to-the-southeast shear zone (Hansen and Dusel-Bacon 1998). These relations lead us to interpret the disturbed  $^{40}\text{Ar}/^{39}\text{Ar}$  age spectrum for sample 23 Hbl (Fig. 8E) as being produced by thermal overprinting of the Early Jurassic contractional episode as a result of strain and fluid interaction associated with mid-Cretaceous extension and perhaps heating from nearby apophyses of the Mount Harper batholith.

The only metamorphic sample from the Molly Creek area with undisturbed  $^{40}\text{Ar}/^{39}\text{Ar}$  systematics (108.4 ± 0.6 Ma Ms plateau age) is Qtz–mica schist sample 21 that crops out west of the Middle Fork of the Fortymile River. Shear-sense indicators in this area record only top-to-the-northwest deformation. A nearly identical Bt plateau age of 106.7 ± 0.6 for post-kinematic Qtz monzonite of the Mount Harper batholith collected 5 km to the north (Fig. 7), is consistent

with the interpretation that the metamorphic cooling age for sample 21 more likely reflects regional uplift and cooling, subsequent to post-kinematic mid-Cretaceous plutonism, rather than the age of the northwest-directed fabric.

### *Central Creek and Salcha River areas*

The Early Jurassic Hbl  $^{40}\text{Ar}/^{39}\text{Ar}$  plateau age of 181.0 ± 6.5 Ma for sample 28 and the Hbl K–Ar age of 188 ± 6 Ma determined for rocks from the inlier of mafic schist and gneiss within the Central Creek augen gneiss body (Fig. 9) indicate that the Early Jurassic metamorphic cooling event, recorded so clearly farther east, probably affected this area as well. The several  $^{40}\text{Ar}/^{39}\text{Ar}$  incremental heating steps with Early Cretaceous ages and large uncertainties determined for sample 28 and the Early Cretaceous step-heating ages determined for nearby sample 29 indicate that more than one thermal event affected the area. The Late Triassic and Jurassic individual step-heating ages determined for sample 33 from the Salcha River gneiss dome are permissive evidence to suggest that the Early Jurassic contractional episode also affected the rocks northwest of the Shaw Creek fault (Fig. 2). In addition, the regional extent of klippe of Seventymile terrane ultramafic rocks, Chatinika assemblage eclogite, and Nisutlin assemblage greenschist-facies rocks indicates a continuity of the structurally high-level assemblages (presumably obducted rocks) across the entire Yukon–Tanana Upland (Fig. 1; Hansen et al. 1991).

Partial replacement of primary Grt by Pl and of Rt by Ilm observed petrographically in sample 28 are consistent with a decompression *P–T* path following a likely high-*P* (>12 kbar) metamorphic episode. Experimental phase equilibria of Ti-phases for the MORB basalt – H<sub>2</sub>O system indicate that Rt is stable at high *P* (>12 kbar), whereas Ilm is stable at lower *P* and moderate to high *T* (Ernst and Liu 1998). The experiments were conducted under conditions that simulate the environment of the upper part of subducting, relatively unaltered oceanic crust (Ernst and Liu 1998). Ernst and Liu caution that the Ti-phase boundaries are sensitive to bulk-rock compositional variations, but point out that the fields are topologically consistent with the natural occurrences of rutile in eclogite + hornblende – eclogite, and ilmenite in granulite + high-rank amphibolite. Although trace element geochemistry of sample 28 resembles that of alkalic basalt (Dusel-Bacon and Cooper 1999), its major element composition is comparable to that of the MORB samples that Ernst and Liu (1998) used to develop the thermobarometer, and hence we feel that our pressure estimate is justified.

One-half kilometre east of sample 28, at the same locality as the amphibolite that gave a 188 ± 6 Ma Hbl K–Ar age, high-*P* metamorphic conditions are also indicated for an unaltered amphibolite that contains the unusual metamorphic mineral assemblage of Pl–Hbl–Grt–Ky–St–Rt. Garnet thermobarometry of that fresh amphibolite (91ADb17A), using a variety of equilibria, indicate that peak metamorphic conditions were in the range of 7–11 kbar and 550–670°C (C. Dusel-Bacon, unpublished data). Pressure–temperature studies of Ky + St + Hbl amphibolites in other high-pressure metamorphic belts of the world indicate *P* of ~9–10 kbar and *T* > 550°C (the lower stability limit of staurolite; Selverstone et al. 1984, p. 514). A different sample of Ky–

St–Grt–Hbl–Pl gneiss (75AWr 198B) at the same locality exhibits greenschist-facies retrograde metamorphic affects (white mica after Ky and Chl after St). We interpret the  $^{40}\text{Ar}/^{39}\text{Ar}$  and petrologic data from the inlier of mafic schist within the Central Creek augen gneiss body to indicate that the mafic rocks experienced high- $P$  amphibolite-facies or hornblende-eclogite-facies metamorphism in the Early Jurassic and were subsequently overprinted by greenschist-facies metamorphism in the Early Cretaceous. Preservation of the older ages indicates that, at least locally, metamorphic temperatures during the subsequent Cretaceous thermal event remained below  $\sim 450^\circ\text{C}$  (the estimated blocking temperature of Hbl). The sample 28 locality records top-to-the-northwest displacement, the inferred direction of Early Jurassic contractional deformation.

The nature of the contact between the inlier of mafic rocks that give the Jurassic metamorphic cooling ages and the surrounding augen gneiss and associated Qtz–mica schist and gneiss of the Lake George assemblage is unknown. Dusel-Bacon and Hansen (1992) previously suggested, on the basis of the Early Jurassic metamorphic cooling ages and high- $P$  metamorphic mineral assemblage, that this area of mafic rocks may be a klippen of Fortymile River assemblage rocks that structurally overlies Lake George assemblage augen gneiss. However, subsequent trace element geochemical data from amphibolites (including our sample 28) from the inlier indicate a within-plate basaltic affinity for their protoliths — an affinity that is typical for many of the Lake George assemblage amphibolites but would be anomalous for Fortymile River assemblage amphibolites (Dusel-Bacon and Cooper 1999). Dusel-Bacon and Cooper (1999), therefore, concluded that the Early Jurassic metamorphic cooling ages from the inlier are better interpreted to reflect cooling of lower plate Lake George assemblage amphibolite during Early Jurassic contraction.

This interpretation of the geologic history of sample 28 is similar to that which we propose for sample 12 that crops out within the fault zone in the northeastern Tanacross quadrangle. Sample 12 gives a Middle Jurassic age of 166 Ma, interpreted as a result of delayed cooling following top-to-the-northwest Early Jurassic contraction. Both samples 28 and 12 experienced intermediate- to high- $P$  amphibolite-facies metamorphic conditions, record top-to-the-northwest shear, and have alkalic within-plate basaltic chemistry, characteristic of many of the amphibolites in the Lake George assemblage. The unusual metamorphic mineral assemblage Grt–Ky–Hbl, present at the Early Jurassic K/Ar age site next to sample 28, is also present in sample 12 for which a  $P$  of 6.5–8.8 kbar was determined (Dusel-Bacon et al. 1995). Other pre-Cretaceous metamorphic cooling ages from lower plate assemblages of the western Yukon–Tanana Upland that are compositionally and stratigraphically similar to the Lake George assemblage, while unusual, have been determined: Newberry et al. (1996) report that amphibolites in the Fairbanks Schist (to the north) yield K–Ar and  $^{40}\text{Ar}/^{39}\text{Ar}$  cooling ages of up to 250 Ma, which they interpret to be cooling from prograde metamorphism, as well as 110–120 Ma ages, which they interpret to be cooling from subsequent retrograde greenschist-facies metamorphism.

Hornblende from sample 30, an amphibolite that records top-to-the-northwest shear and crops out at the base of the

small ultramafic body that overlies augen gneiss, gives a well-defined Early Cretaceous ( $120.4 \pm 0.7$  Ma) metamorphic cooling age. Approximately 3 km south of sample 30, Hbl from another amphibolite associated with a smaller metamorphosed ultramafic body gave a K–Ar age of  $132.6 \pm 1.8$  Ma (Fig. 9; Wilson et al. 1985). Shear-sense indicators measured at this locality, like those from all but one kinematic locality in the Central Creek area (Fig. 9), indicate top-to-the-west-northwest tectonic transport. This correspondence between metamorphic cooling ages and tectonic vergence in amphibolites associated with the small ultramafic bodies and those in the schist and gneisses of the Lake George assemblage indicates a shared metamorphic and tectonic history during the latest dynamothermal event. These data are consistent with the observation that these small ultramafic bodies, unlike the larger ultramafic klippe of the Seventymile terrane (Foster 1992), are infolded with amphibolite-facies gneiss and schist and that some peridotite contains a metamorphic mineral assemblage consisting of Amp, Chl, Mag, and Atg (Weber et al. 1978).

High- $P$  conditions during metamorphism of metabasaltic rocks at the base of the largest of the small ultramafic bodies are indicated by (1) mineral chemistry of Hbl in both Grt amphibolite that underlies the ultramafic and in sample 30 collected from a concordant amphibolite layer  $\sim 5$ – $10$  m lower in the section, and (2) reaction textures observed in the Grt amphibolite. Hbl grains from sample 30 average 13 wt.%  $\text{Al}_2\text{O}_3$  and 0.7 wt.%  $\text{TiO}_2$ , and Hbl from the Grt amphibolite that immediately overlies sample 30 (sample 91ADb 21A) average 16 wt.%  $\text{Al}_2\text{O}_3$  and 0.3 wt.%  $\text{TiO}_2$  (Dusel-Bacon, unpub. data, 2000). Applying the semiquantitative Ca-amphibole thermobarometer of Ernst and Liu (1998), these contents correspond to  $P$ – $T$  conditions of  $\sim 15$  kbar at  $650^\circ\text{C}$  and  $\sim 22$  kbar at  $< 600^\circ\text{C}$ , respectively. Thin sections of the overlying Grt amphibolite show complex reaction textures consisting of coarse-grained Grt and medium- to fine-grained Hbl and Ap; a reactant assemblage of Bt, Czo/Zo; and an extremely fine-grained symplectite of intergrown sodic Pl, less aluminous Hbl (than the coarser grained Hbl), and Cpx. Although sodic pyroxene (omphacite), which would constitute clear evidence for an earlier eclogite-facies metamorphic event, was not observed in thin section, textural evidence is consistent with high- $P$  and  $-T$  metamorphism of an aluminous basalt or gabbro protolith, followed by retrogressive (decompression?) amphibolite-facies metamorphism. The bulk composition of the large patches of symplectite surrounding Grt are a reasonable approximation of the composition of omphacite, and locally preserved Rt crystals rimmed by Ilm attest to a decrease in pressure from  $> 12$  kbar (stability field of Rt for the MORB basalt –  $\text{H}_2\text{O}$  system; Ernst and Liu 1998) to lower  $T$  and  $P$  amphibolite-facies conditions. The fact that sample 30, which probably experienced a pre-Cretaceous high- $P$  and  $-T$  metamorphism, now gives a Cretaceous  $^{40}\text{Ar}/^{39}\text{Ar}$  metamorphic cooling age suggests that metamorphic  $T$  during the late-phase, or subsequent retrograde, episode exceeded the estimated  $\sim 450^\circ\text{C}$  closure temperature of Hbl. This proposed complete Cretaceous overprinting of a previous dynamothermal episode is consistent with the higher  $T$  retrograde assemblage (i.e., including Bt) in the Grt amphibolite relative to that preserved locally in retrograded

amphibolite associated with the inlier of mafic rocks that gives the Early Jurassic metamorphic cooling ages. These observations support the interpretation, previously proposed by Dusel-Bacon and Hansen (1992), that the small masses of ultramafic rocks in the Central Creek area were initially metamorphosed deep within a west-dipping subduction zone that resulted in the collision and imbrication of the oceanic rocks with the continental margin rocks of the Lake George assemblage.

Other Early Cretaceous metamorphic cooling ages in the southeastern Big Delta area (Fig. 9) fall in the approximate same range as those determined for Lake George assemblage rocks in the eastern Yukon–Tanana Upland (Fig. 3): Hbl  $^{40}\text{Ar}/^{39}\text{Ar}$  ages are between ~135–120 Ma, and Ms and Bt  $^{40}\text{Ar}/^{39}\text{Ar}$  ages are ~110–108 Ma (Fig. 9). Titanite from augen gneiss in the eastern part of the Central Creek augen gneiss body gave a ~134 Ma U–Pb conventional age for a single fraction (Aleinikoff et al. 1981; Fig. 9), but as discussed earlier in the text, interpretation of this age is ambiguous.

Although the similarity between  $^{40}\text{Ar}/^{39}\text{Ar}$  ages of Bt and Ms in some metamorphic samples with those in nearby plutons allows the possibility that some of the ages were reset by hydrothermal circulation or conductive heating associated with the Early Cretaceous plutons, we consider it more likely that the Cretaceous metamorphic ages record regional uplift and cooling following Early Cretaceous deformation for the following reasons: (1) similar metamorphic cooling ages occur in rocks distant from plutons (e.g., localities 13, 14, 15, 16, 17, 31, 32) and in rocks located relatively close to them (within a distance equal to the radius or half-width of the pluton); (2) metamorphic rocks with Early Cretaceous metamorphic cooling ages generally exhibit metamorphic textures that indicate that deformation continued during cooling. A maximum age for the deformation that we propose accompanied the Early Cretaceous metamorphic cooling in the Central Creek area is provided by a preliminary 128 Ma U–Pb Zrn igneous crystallization age of an orthogneiss collected ~5 km southeast of the Pogo gold property (Fig. 9) in the northwestern part of our study area (Smith et al. 1999; J.R. Bressler, oral communication, 2000).

We interpret the Early Cretaceous  $^{40}\text{Ar}/^{39}\text{Ar}$  metamorphic cooling ages of  $113.6 \pm 2.8$  Ma (Hbl; sample 32),  $109.3 \pm 0.6$  (Bt; sample 32), and  $109.6 \pm 0.6$  (Ms; sample 34) from schists within the eastern margin of the Salcha River gneiss dome, near the inferred detachment zone that separates the high-grade rocks of the dome from lower grade rocks of the overlying Nisutlin assemblage (Fig. 2), to indicate the time at which the high-grade footwall rocks cooled from ~450°C through ~300°C during the episode of southeast-vergent extension and associated exhumation proposed by Pavlis et al. (1993). Decompression melting likely accompanied extension and formation of the Salcha River gneiss dome, as suggested by (1) the presence of andalusite-bearing Qtz veins and partial melts within the core of the gneiss dome (Dusel-Bacon and Foster 1983; Sisson et al. 1990), and (2) the closeness in age between the ~115 Ma U–Pb Zrn crystallization age of a small intrusion within the dome (Aleinikoff et al. 1984) and the  $113.6 \pm 2.8$  Ma Hbl  $^{40}\text{Ar}/^{39}\text{Ar}$  cooling age of sample 32. The cooling ages of the  $^{40}\text{Ar}/^{39}\text{Ar}$  Hbl–Bt pair from sample 32 indicate a moderate cooling rate of ~40°C/Ma

from ~450 to ~300°C, a rate difficult to associate with a single tectonic process.

It is unclear whether the northwest-vergent deformation and Early Cretaceous syntectonic metamorphic cooling (from ~450 to 300°C) in the Central Creek area took place under contractional or extensional conditions. In the absence of other information, we interpret the metamorphic and tectonic history of the Central Creek area to be analogous with that of the Molly Creek and eastern Eagle – Tanacross areas to the east and the Salcha River gneiss dome to the northwest: Early Jurassic margin-parallel obduction of outboard oceanic rocks of the Seventymile assemblage and distal continental-margin rocks onto the continental margin rocks of the Lake George assemblage, crustal thickening and metamorphism of all assemblages, and Early Cretaceous exhumation and cooling of the structurally deeper Lake George assemblage. A possible explanation for the absence of the southeast-vergent extensional structures present elsewhere in the region is that the level of exposure of the Central Creek augen gneiss body is deeper (suggested by a larger and more continuous exposure of augen gneiss) than that which is present in the Salcha River gneiss dome and northeastern Tanacross quadrangle, and thus, detachment structures with southeast-vergence may have originally overlain the Central Creek augen gneiss but have since been eroded away.

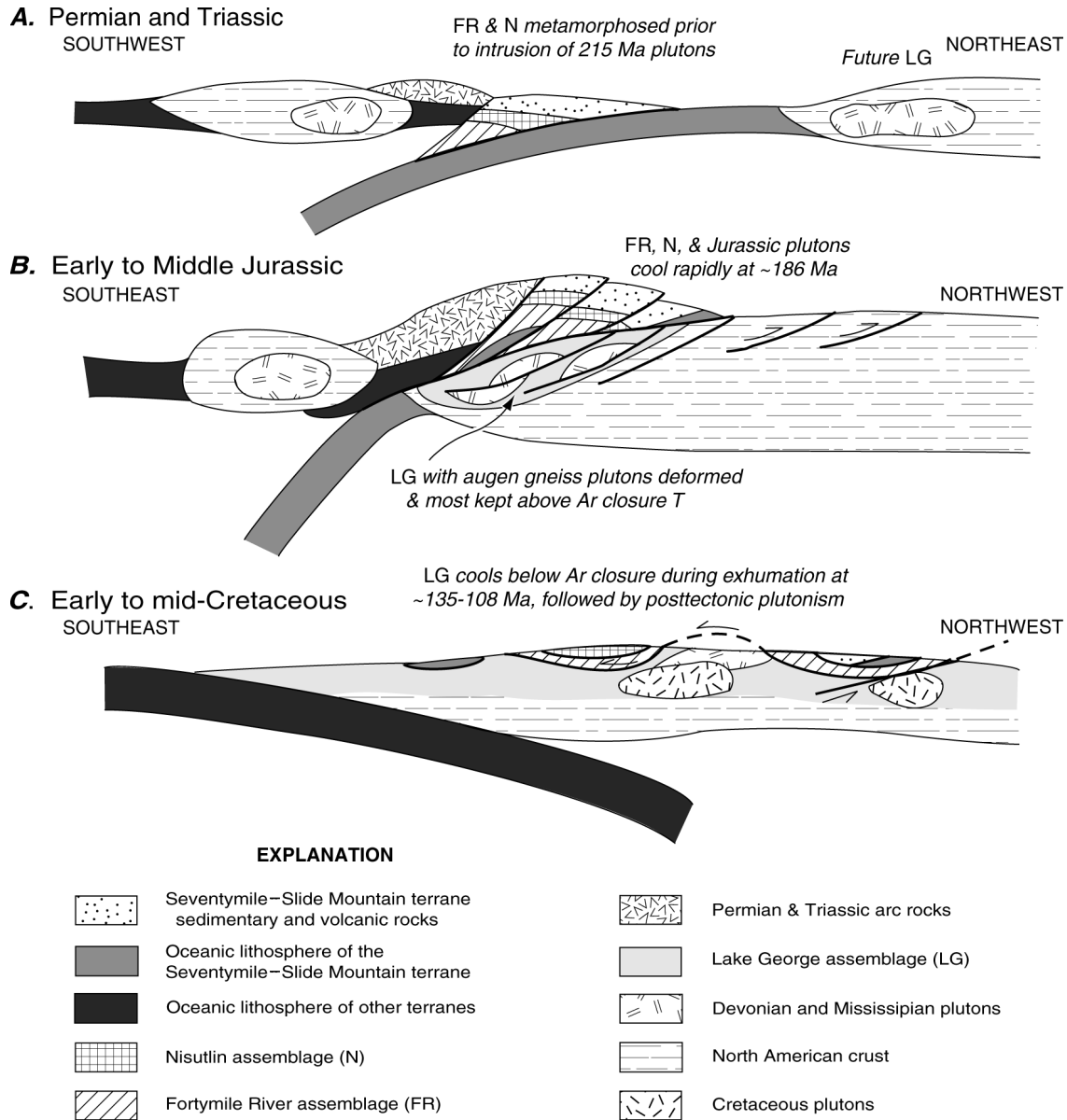
The ~107 Ma  $^{40}\text{Ar}/^{39}\text{Ar}$  Bt and Ms ages for the posttectonic Harper Mountain – Black Mountain batholith (Figs. 7, 9) east of the Central Creek augen gneiss body indicate a simultaneous and regional cooling below ~300°C of both the posttectonic Early Cretaceous batholith and the Lake George assemblage country rocks. U–Pb dating of the Early Cretaceous plutons is necessary to determine the timing between igneous crystallization and regional uplift of these plutons, but it would not be unexpected to have the crustal melting to form granitoids facilitated by decreasing  $P$  during the later stages of extension-related exhumation, as previously proposed by Dusel-Bacon et al. (1995).

## Tectonic model

Thermochronologic, petrologic, and kinematic data from east-central Alaska and Yukon Territory are consistent with the tectonic model proposed by Hansen (1990) and Hansen et al. (1991) whose pre-mid-Cretaceous components are based, to a large degree, on the hypothesis of a rifted continental margin and an arc-continent collision made by Tempelman-Kluit (1979) (see Hansen and Dusel-Bacon 1998 for discussion). According to this model, Devonian to Mississippian rifting along the western margin of North America formed the Anvil Ocean (oceanic crust to form the future Seventymile – Slide Mountain terrane). Prior to rifting, or perhaps, in some cases, related to it, Devonian–Mississippian granitoids intruded both the continental margin (we interpret to include the Lake George assemblage) and the rifted fragment of North American crust (Nisling terrane; Fig. 1) and adjacent marginal basin sediments and volcanics (Fortymile River and Nisutlin assemblages).

By Middle Permian time (Fig. 11A), southwest-dipping, right-oblique subduction of the Anvil Ocean lithosphere had begun (Hansen 1989). Low- $P$  and - $T$  metamorphism of the Nisutlin assemblage, moderate- to high- $P$  and  $T$  meta-

**Fig. 11.** Simplified tectonic model for Permian to mid-Cretaceous thermal and deformational evolution of east-central Alaska. Modified from Hansen et al. (1991). See text for explanation, and Hansen et al. (1991), Dusel-Bacon et al. (1995), and Hansen and Dusel-Bacon (1998) for a more complete discussion of some of the data used in developing this model. *T*, temperature.



morphism of the Fortymile River assemblage, and high-*P* metamorphism of most occurrences of eclogite and blueschist shown on Fig. 1, formed at increasing depths within the subduction zone. Middle Permian metavolcanic and metaplutonic rocks in western Yukon and easternmost Alaska likely represent part of the calc-alkaline arc developed over the subduction zone that brought Permian eclogite and outboard assemblages (Fortymile River and Nisutlin assemblages, and Seventymile – Slide Mountain terrane) onto the continental margin of North America (e.g., Mortensen 1990, 1992; Hansen et al. 1991; Creaser et al. 1997). Concordant U–Pb ages of  $269 \pm 2$  Ma for metamorphic zircons from eclogite near Last Peak in the Teslin suture zone of southern Yukon (Teslin tectonic zone of Stevens et al. 1996) and near St. Cyr, ~75 km to the east, (Creaser et al. 1997; Erdmer et al. 1998) provide strong evidence that high-*P*

metamorphism, and hence subduction, was going on in Middle Permian time. Subduction continued in Late Triassic to Early Jurassic time as evidenced by arc granitoids of this age in the Fortymile River and Nisutlin assemblages in Alaska and comparable Yukon–Tanana terrane assemblages, as well as the Nisling and Stikine terranes in the Yukon (Johnston et al. 1996). It is important to note that there are no documented examples of Late Triassic to Early Jurassic calc-alkaline plutons that intrude the Lake George assemblage or the Cassiar terrane (Fig. 1), which according to our model (Fig. 11A), are parautochthonous North American strata that originated east of the Anvil Ocean. Although plutons just east of the Alaska–Yukon border (Crag Mountain and adjacent plutons) that intrude the continuation of the Lake George assemblage are shown to be Early Jurassic on regional compilations (Mortensen 1996; Mortensen et al.

2000; Gordey and Makepeace 2001), recent U–Pb monazite data indicate that they are, instead, Cretaceous in age (J.K. Mortensen, written communication, 2001). The late- to posttectonic timing of intrusion of the Late Triassic to Early Jurassic plutons is compatible with the hypothesis of Hansen (1992a) that tectonites were progressively underplated onto the hanging wall; hence an arc might be expected to intrude previously deformed and underplated tectonites formed earlier during an ongoing subduction process.

According to our model (Fig. 11B), the Early Jurassic (~188–186 Ma)  $^{40}\text{Ar}/^{39}\text{Ar}$  ages from metamorphic tectonites and plutonic rocks in the eastern Eagle quadrangle, date the time of regional cooling following northwest-directed contraction that emplaced the Fortymile River assemblage onto the Nasina assemblage to the north and the Lake George assemblage to the south. Cooling of the upper plate assemblages was the final stage of a continuum of subduction-related contraction that produced crustal thickening and intermediate- to high- $P$  metamorphism within both the Fortymile River assemblage and the structurally underlying Lake George assemblage. U–Pb data indicate a similar history involving arc plutonism and rapid exhumation of the Aishihak metamorphic suite (part of the Nisling terrane in southwest Yukon) at about 186 Ma (Johnston et al. 1996). Elsewhere in southern Yukon, metamorphic cooling ages from upper plate assemblages span a wider range: In the Laberge – Quiet Lake area of the Teslin suture zone, upper plate high- $P$ – $T$  (Hansen 1992b) tectonites cooled rapidly at ~195 Ma, as a result of collision and exhumation (Hansen et al. 1991).  $^{40}\text{Ar}/^{39}\text{Ar}$  cooling ages for white mica from eclogite and blueschist localities in central Yukon (Fig. 1) record ongoing Mississippian, Permian, and Middle Triassic subduction and cooling (Erdmer et al. 1998).

We interpret the Early Cretaceous metamorphic cooling ages in the eastern Lake George assemblage, and perhaps in much of the lower plate assemblage, to reflect cooling and exhumation as a result of crustal extension that followed, by some 50 Ma, obduction of the overlying terranes (Fig. 11C; e.g., Hansen et al. 1991; Pavlis et al. 1993). This crustal extension may have been a byproduct of the subsequent development of a north- to northeast-dipping subduction system outboard of the collapsed margin, which eventually resulted in the accretion of the Peninsular–Wrangellia–Alexander superterrane to the Early Cretaceous North American continental margin (Pavlis et al. 1993). Early Cretaceous tectonism, possibly including prograde metamorphism in some areas, was closely followed by posttectonic plutonism at ~108 Ma, perhaps as a result of melting facilitated by decreasing  $P$  during the later stages of exhumation.

## Acknowledgments

We are indebted to Charlie Bacon for assistance in the field, electron microprobe analyses of mineral separates, and preparation of the  $^{40}\text{Ar}/^{39}\text{Ar}$  spectra figures. Sue Douglass prepared many of the dated mineral separates. Scott McPeck and Judy Weathers expertly and patiently took the map figures through numerous iterations. Warren Nokleberg allowed us to publish the  $^{40}\text{Ar}/^{39}\text{Ar}$  results for four samples he and colleagues collected during the Trans Alaska Crustal

Transect project. Mark Harrison is also thanked for his analysis of one of the samples when the  $^{40}\text{Ar}/^{39}\text{Ar}$  technique was first applied to Yukon–Tanana rocks. Rob McDonald of TECK Corporation and Patrick Smith of Kennecott Exploration generously provided industry reports dealing with the geology of the Napoleon Creek gold property. We thank Rainer Newberry and Dwight Bradley for helpful comments to an earlier version of this manuscript and Canadian Journal of Earth Sciences (CJES) reviewers John Aleinikoff and Mike Villeneuve for improving this manuscript.

## References

- Alaska Division of Geological and Geophysical Surveys. 1999. Total field magnetics of part of the Fortymile Mining District, Alaska (southern Eagle and northern Tanacross quadrangles. Report of Investigations 99-1 (2 sheets); scale 1 : 63 360.
- Aleinikoff, J.N., Dusel-Bacon, C., and Foster, H.L. 1981. Geochronologic studies in the Yukon–Tanana Upland, east-central Alaska. *In* The United States Geological Survey in Alaska: Accomplishments during 1979. *Edited by* N.R.D. Albert and T. Hudson. U.S. Geological Survey, Circular 823-B, pp. 34–37.
- Aleinikoff, J.N., Dusel-Bacon, C., and Foster, H.L. 1984. Uranium–lead isotopic ages of zircon from sillimanite gneiss, east-central Alaska, and implications for Paleozoic metamorphism, Big Delta quadrangle. *In* The United States Geological Survey in Alaska: Accomplishments during 1981. *Edited by* W.L. Coonrad and R. I. Elliott. U.S. Geological Survey, Circular 868, pp. 45–48.
- Aleinikoff, J.N., Dusel-Bacon, C., Foster, H.L., and Nokleberg, W.J. 1987. Lead isotopic fingerprinting of tectono-stratigraphic terranes, east-central Alaska. *Canadian Journal of Earth Sciences*, **24**: 2089–2098.
- Bacon, C.R., Foster, H.L., and Smith, J.G. 1990. Rhyolitic calderas of the Yukon–Tanana terrane, east-central Alaska: Volcanic remnants of a mid-Cretaceous magmatic arc. *Journal of Geophysical Research*, **95**(B13): 21 451 – 21 461.
- Baldwin, S.L., Harrison, T.M., and FitzGerald, J.D. 1990. Diffusion of  $^{40}\text{Ar}$  in metamorphic hornblende. *Contributions to Mineralogy and Petrology*, **105**: 691–703.
- Coney, P.J., Jones, D.L., and Monger, W.H. 1980. Cordilleran suspect terranes. *Nature (London)*, **288**: 329–333.
- Creaser, R.A., Heaman, L.M., and Erdmer, P. 1997. Timing of high-pressure metamorphism in the Yukon–Tanana terrane, Canadian Cordillera: constraints from U–Pb zircon dating of eclogite from the Teslin tectonic zone. *Canadian Journal of Earth Sciences*, **34**: 709–715.
- Cushing, G.W. 1984. The tectonic evolution of the eastern Yukon–Tanana upland. Unpublished M.Sc. thesis, State University of New York, Albany, N.Y.
- Dalrymple, G.B. 1989. The GLM continuous laser system for  $^{40}\text{Ar}/^{39}\text{Ar}$  dating: Description and performance characteristics. U.S. Geological Survey, Bulletin 1890, pp. 89–96.
- Day, W.C., Gamble, B.M., Henning, M.W., and Smith, B.D. 2000. Geologic setting of the Fortymile River area — polyphase deformational history within part of the eastern Yukon–Tanana uplands of Alaska. *In* Geologic studies in Alaska by the U.S. Geological Survey 1998. *Edited by* K.D. Kelly and L.P. Gough. U.S. Geological Survey, Professional Paper 1615, pp. 65–82.
- Duffield, W.A., and Dalrymple, G.B. 1990. The Taylor Creek Rhyolite of New Mexico: a rapidly emplaced field of lava domes and flows. *Bulletin of Volcanology*, **52**: 475–487.
- Dusel-Bacon, C., and Aleinikoff, J.N. 1985. Petrology and tectonic significance of augen gneiss from a belt of Mississippian

- granitoids in the Yukon–Tanana terrane, east-central Alaska. *Geological Society of America Bulletin*, **96**: 411–425.
- Dusel-Bacon, C., and Aleinikoff, J.N. 1996. U–Pb zircon and titanite ages for augen gneiss from the Divide Mountain area, eastern Yukon–Tanana upland, Alaska, and evidence for the composite nature of the Fiftymile Batholith. *In* *Geologic studies in Alaska by the U.S. Geological Survey during 1994. Edited by T.E. Moore and J.A. Dumoulin*. U.S. Geological Survey, Bulletin 2152, pp. 131–141.
- Dusel-Bacon, C., and Cooper, K.M. 1999. Trace-element geochemistry of metabasaltic rocks from the Yukon–Tanana Upland and implications for the origin of tectonic assemblages in east-central Alaska. *Canadian Journal of Earth Sciences*, **36**: 1671–1695.
- Dusel-Bacon, C., and Foster, H.L. 1983. A sillimanite gneiss dome in the Yukon crystalline terrane, east-central Alaska: Petrography and garnet-biotite geothermometry. U.S. Geological Survey, Professional Paper 1170-E.
- Dusel-Bacon, C., and Hansen, V.L. 1992. High-pressure amphibolite-facies metamorphism and deformation within the Yukon–Tanana and Taylor Mountain terranes, eastern Alaska. *In* *Geologic studies in Alaska by the U.S. Geological Survey 1991. Edited by D.C. Bradley and C. Dusel-Bacon*. U.S. Geological Survey, Bulletin 2041, pp. 140–159.
- Dusel-Bacon, C., and Murphy, J.M. 2001. Apatite fission-track evidence of widespread Eocene heating and exhumation in the Yukon–Tanana Upland, interior Alaska. *Canadian Journal of Earth Sciences*, **38**: 1191–1204.
- Dusel-Bacon, C., Csejtey, B., Foster, H.L., Doyle, E.O., Nokleberg, W.J., and Plafker, G. 1993. Distribution, facies, ages, and proposed tectonic associations of regionally metamorphosed rocks in east- and south-central Alaska. U.S. Geological Survey, Professional Paper 1497-C, scale 1 : 1 000 000.
- Dusel-Bacon, C., Hansen, V.L., and Scala, J.A. 1995. High-pressure amphibolite facies dynamic metamorphism and the Mesozoic tectonic evolution of an ancient continental margin, east-central Alaska. *Journal of Metamorphic Geology*, **13**: 9–24.
- Dusel-Bacon, C., Bressler, J.R., Takaoka, H., Mortensen, J.K., Oliver, D.H., Leventhal, J.S., Newberry, R.J., and Bundtzen, T.K. 1998. Stratiform zinc–lead mineralization in Nasina assemblage rocks of the Yukon–Tanana Upland in east-central Alaska. U.S. Geological Survey, Open-File Report 98-340 (<http://geopubs.wr.usgs.gov/open-file/of98-340/>).
- Erdmer, P., Ghent, E.D., Archibald, D. A., and Stout, M.Z. 1998. Paleozoic and Mesozoic high-pressure metamorphism at the margin of ancestral North America in central Yukon. *Geological Society of America Bulletin*, **110**: 615–629.
- Ernst, W.G., and Liu, J. 1998. Experimental phase-equilibrium study of Al- and Ti-contents of calcic amphibole in MORB — A semiquantitative thermobarometer. *American Mineralogist*, **83**: 952–969.
- Fleck, R.J., Sutter, J.F., and Elliot, D.H. 1977. Interpretation of discordant  $^{40}\text{Ar}/^{39}\text{Ar}$  age-spectra of Mesozoic tholeiites from Antarctica. *Geochimica et Cosmochimica Acta*, **41**: 15–32.
- Foster, H.L. 1969. Reconnaissance geology of the Eagle A-1 and A-2 quadrangles, Alaska. U.S. Geological Survey, Bulletin 1271-G, scale 1 : 63 360.
- Foster, H.L. 1976. Geologic map of the Eagle quadrangle, Alaska. U.S. Geological Survey, Miscellaneous Geologic Investigations Series Map I-922, scale 1 : 250 000.
- Foster, H.L. 1992. Geologic map of the eastern Yukon–Tanana region, Alaska. U.S. Geological Survey, Open-File Report 92-313, scale 1 : 500 000.
- Foster, H.L., Cushing, G. W., and Keith, T. E. C. 1985. Early Mesozoic tectonic history of the boundary area, east-central Alaska. *Geophysical Research Letters*, **12**: 553–556.
- Foster, H.L., Keith, T.E.C., and Menzie, W.D. 1994. Geology of the Yukon–Tanana area of east-central Alaska. *In* *The geology of Alaska. Edited by G. Plafker and H.C. Berg*. Geological Society of America, Boulder, Colo., *The Geology of North America*, G-1, pp. 197–217.
- Frost, B.R., Chamberlain, K.R., and Schumacher, J.C. 2000. Sphene (titanite): phase relations and role as a geochronometer. *Chemical Geology*, **172**: 131–148.
- Gordey, S.P., and Makepeace, A.J. (Compilers) 2001. Bedrock geology, Yukon Territory. Geological Survey of Canada, Open File 3754, and Exploration and Geological Services Division, Yukon, Indian and Northern Affairs Canada, Open File 2001-1, scale 1 : 1 000 000.
- Hansen, V.L. 1989. Structural and kinematic evolution of the Teslin suture zone, Yukon: record of an ancient transpressional margin. *Journal of Structural Geology*, **11**: 717–733.
- Hansen, V.L. 1990. Yukon–Tanana terrane: A partial acquittal. *Geology*, **18**: 365–369.
- Hansen, V.L. 1992a. Backflow and margin-parallel shear within an ancient subduction complex. *Geology*, **20**: 71–74.
- Hansen, V.L. 1992b. P–T evolution of the Teslin suture zone and Cassiar tectonites, Yukon, Canada: evidence for A- and B-type subduction. *Journal of Metamorphic Geology*, **10**: 239–263.
- Hansen, V.L., and Dusel-Bacon, C. 1998. Structural and kinematic evolution of the Yukon–Tanana upland tectonites, east-central Alaska: A record of late Paleozoic to Mesozoic crustal assembly. *Geological Society of America Bulletin*, **110**: 211–230.
- Hansen, V.L., Heizler, M.T., and Harrison, T.M. 1991. Mesozoic thermal evolution of the Yukon–Tanana composite terrane: New evidence from  $^{40}\text{Ar}/^{39}\text{Ar}$  data. *Tectonics*, **10**: 51–76.
- Harrison, T.M., and Fitzgerald, J.D. 1986. Exsolution in hornblende and its consequences for  $^{40}\text{Ar}/^{39}\text{Ar}$  age spectra and closure temperature. *Geochimica et Cosmochimica Acta*, **50**: 247–253.
- Harrison, T.M., Duncan, I., and McDougall, I. 1985. Diffusion of  $^{40}\text{Ar}$  in biotite: temperature, pressure and compositional effects. *Geochimica et Cosmochimica Acta*, **49**: 2461–2468.
- Heslop, K., Dusel-Bacon, C., Williams, I.S. 1995. Survival of zircon U–Pb isotopic systems through partial melting and high P–T dynamothermal metabolism, Yukon–Tanana terrane, Alaska. *Geological Society of America, Abstracts with Programs*, **27**: 26.
- Hunziker, J.C., Desmons, J., and Hurford, A.J. 1992. Thirty-two years of geochronological works in the central and western Alps: A review on seven maps. *Memoires de Geologie*, **13**: 1–59. University of Lausanne, Lausanne, Switzerland.
- Johnston, S.T., Mortensen, J.K., and Erdmer, P. 1996. Igneous and metaigneous age constraints for the Aishihik metamorphic suite, southwest Yukon. 1996. *Canadian Journal of Earth Sciences*, **33**: 1543–1555.
- Kretz, R. 1983. Symbols for rock-forming minerals. *American Mineralogist*, **68**: 277–279.
- Lanphere, M.A. 2000. Comparison of conventional K–Ar and  $^{40}\text{Ar}/^{39}\text{Ar}$  dating of young mafic volcanic rocks. *Quaternary Research*, **53**: 294–301.
- Layer, P.W. 2000. Argon-40/argon-39 age of the El'gygytyn impact event, Chukotka, Russia. *Meteoritics and Planetary Science*, **35**: 591–599.
- Ludwig, K.R. 2000. Isoplot/Ex, A geochronological tool kit for Microsoft Excel version 2.2. Berkeley Geochronology Center, Special Publication 1a.

- McDougall, I., and Harrison, T.M. 1999. 2nd ed. Geochronology and thermochronology by the  $^{40}\text{Ar}/^{39}\text{Ar}$  method. Oxford University Press, Oxford, U.K.
- Mertie, J.B., Jr. 1930. Geology of the Eagle–Circle district, Alaska. U.S. Geological Survey Bulletin 816.
- Min, K., Mundil, R., Renne, P., and Ludwig, K.R. 2000. A test for systematic errors in  $^{40}\text{Ar}/^{39}\text{Ar}$  geochronology through comparison with U–Pb analysis of a 1.1 Ga rhyolite. *Geochemica et Cosmochemica Acta*, **64**: 73–98.
- Mortensen, J.K. 1988. Geology of southwestern Dawson map area. Geological Survey of Canada Open-File 1927, scale 1 : 250 000.
- Mortensen, J.K. 1990. Geology and U–Pb geochronology of the Klondike District, west-central Yukon Territory: *Canadian Journal of Earth Sciences*, **27**: 903–914.
- Mortensen, J.K. 1992. Pre-mid-Mesozoic tectonic evolution of the Yukon–Tanana terrane, Yukon and Alaska. *Tectonics*, **11**: 836–853.
- Mortensen, J.K. 1996. Geological compilation map of the northern Stewart River map area, Klondike and Sixtymile Districts, Yukon: Exploration and Geological Services Division, Yukon, Indian and Northern Affairs Canada, Geoscience Map 1999-1, 6 sheets, scale 1 : 50 000.
- Mortensen, J.K., Emon, K., Johnston, S.T., and Hart, C.J.R. 2000. Age, geochemistry, paleotectonic setting and metallogeny of Late Triassic – Early Jurassic intrusions in the Yukon and eastern Alaska: a preliminary report. *In* Yukon Exploration and Geology 1999. Edited by D.S. Emond and L.H. Weston. Exploration and Geological Services Division, Yukon, Indian and Northern Affairs Canada: pp. 139–144.
- Newberry, R.J., Layer, P.W., Solie, D.N., and Burleigh, R.E. 1995a. Mesozoic–Tertiary igneous rocks of eastern interior Alaska: Ages, compositions, and tectonic setting. *Geological Society of America, Abstracts with Programs*, **27**: 68.
- Newberry, R.J., Solie, D.N., Burns, L.E., Wiltse, M.A., Hammond, R.J., and Swainbank, R. 1995b. Geophysical and geological evidence for pervasive, northeast-trending, left-lateral faults in eastern interior Alaska. *Geological Society of America, Abstracts with Programs*, **27**: 68.
- Newberry, R.J., Bundtzen, T.K., Clautice, K.H., Combellick, R.A., Douglas, T., Laird, G.M., Liss, S.A., Pinney, D.S., Reifenhuth, R.R., and Sole, D.N. 1996. Preliminary Geologic Map of the Fairbanks Mining District, Alaska. Alaska Division of Geological and Geophysical Surveys, Public Data File 96-16, 2 sheets, scale 1 : 63 360.
- Newberry, R.J., Bundtzen, T.K., Mortensen, J.K., and Weber, F.R. 1998a. Petrology, geochemistry, age, and significance of two foliated intrusions in the Fairbanks District, Alaska. *In* Geologic Studies in Alaska by the United States Geological Survey 1996. Edited by J.E. Gray and J.R. Riehle. U.S. Geological Survey, Professional Paper 1595, pp. 117–129.
- Newberry, R.J., Layer, P.W., Burleigh, R.E., and Solie, D.N. 1998b. New  $^{40}\text{Ar}/^{39}\text{Ar}$  dates for intrusions and mineral prospects in the eastern Yukon–Tanana Terrane, Alaska. *In* Geologic studies in Alaska by the U.S. Geological Survey 1996. Edited by J.E. Gray and J.R. Riehle. U.S. Geological Survey, Professional Paper 1595, pp. 131–160.
- Nokleberg, W.J., Foster, H.L., and Aleinikoff, J.N. 1989. Geology of the northern Copper River Basin, eastern Alaska Range, and southern Yukon–Tanana Basin, southern and east-central Alaska. *In* Alaskan Geological and Geophysical Transect, Field trip guidebook T104. Edited by W.J. Nokleberg and M.A. Fisher. American Geophysical Union, Washington, D.C., pp. 34–63.
- Okulitch, A.V. 1999. Geological time scale 1999. Geological Survey of Canada, Open File 3040 (National Earth Science Series, Geological Atlas) — Revision.
- Page, R.A., Plafker, G., and Pulpan, H. 1995. Earthquakes and block rotation in east-central Alaska. *Geological Society of America, Abstracts with Programs*, **27**: 70.
- Passchier, C.W., and Trouw, R.A.J. 1996. *Microtectonics*. Springer-Verlag Berlin Heidelberg, Germany.
- Pavlis, T.L., Sisson, V.B., Foster, H.L., Nokleberg, W.J., and Plafker, G. 1993. Mid-Cretaceous extensional tectonics of the Yukon–Tanana terrane, Trans-Alaskan Crustal Transect (TACT), east-central Alaska. *Tectonics*, **12**: 103–122.
- Pidgeon, R.T., Bosch, D., Bruguier, O. 1996. Inherited zircon and titanite U–Pb systems in an Archaean syenite from southwestern Australia: implications for U–Pb stability of titanite. *Earth and Planetary Science Letters*, **141**: 187–198.
- Poulton, T., Orchard, M.J., Gordey, S.P., and Davenport, P. (Compilers). 1999. Yukon fossil determinations. *In* Yukon digital geology. Compiled by S.P. Gordey and A.J. Makepeace. Geological Survey of Canada, Open File D 3826, and Exploration and Geological Services Division, Yukon, Indian and Northern Affairs Canada, Open File 1999-1D.
- Silverstone, J., Spear, F.S., Franz, G., and Morteani, G. 1984. High-pressure metamorphism in the Tauern window, Austria: *P–T* paths from hornblende–kyanite–staurolite schists. *Journal of Petrology*, **25**(part 2): 501–531.
- Sharp, W.D., Turrin, B.D., Renne, P.R., and Lanphere, M.A. 1996.  $^{40}\text{Ar}/^{39}\text{Ar}$  and K–Ar dating of lavas from the Hilo 1-km corehole, Hawaii Scientific Drilling Project. *Journal of Geophysical Research*, **101**: 11607–11616.
- Sharp, W.D., Tobisch, O.T., and Renne, P.R. 2000. Development of Cretaceous transpressional cleavage synchronous with batholith emplacement, central Sierra Nevada, California. *Geological Society of America Bulletin*, **112**: 1059–1066.
- Sisson, V.B., Pavlis, T.L., and Dusel-Bacon, C. 1990. Metamorphic constraints on Cretaceous crustal extension in the Yukon Crystalline terrane, east-central Alaska. *Geological Association of Canada/Mineralogical Association of Canada, Programs with Abstracts*, **15**: A-122.
- Smith, M., Thompson, J.F.H., Bressler, J., Layer, P., Mortensen, J.K., Abe, I., and Takaoka, H. 1999. Geology of Liese Zone, Pogo property, east-central Alaska. *SEG Newsletter*, No. 38.
- Spurr, J.E., 1898. Geology of the Yukon gold district, Alaska. U.S. Geological Survey Annual Report, 18, part 3, pp. 87–392.
- Stevens, R.A., Erdmer, P., Creaser, R.A., and Grant, S.L. 1996. Mississippian assembly of the Nisutlin assemblage: evidence from primary contact relationships and Mississippian magmatism in the Teslin tectonic zone, part of the Yukon–Tanana terrane of south-central Yukon. *Canadian Journal of Earth Sciences*, **33**: 103–116.
- Szumigala, D.J., Newberry, R.J., Weldon, M.B., Finseth, B.A., Pinney, D.S., and Flynn, R.L. 2000a. Major-oxide, minor-oxide, trace-element, and geochemical data from rocks collected in a portion of the Fortymile Mining District, Alaska. State of Alaska Division of Geological and Geophysical Surveys, Raw-Data File 2000-1.
- Szumigala, D.J., Newberry, R.J., Weldon, M.B., Finseth, B.A., and Pinney, D.S. 2000b. Preliminary bedrock geologic map of a portion of the Fortymile Mining District, Alaska. Alaska Division of Geological and Geophysical Surveys, Preliminary Interpretive Report 2000-6, scale 1 : 63 360.
- Tempelman-Kluit, D.J. 1979. Transported cataclasite, ophiolite and granodiorite in Yukon: evidence of arc-continent collision. Geological Survey of Canada, Paper 79-14.
- Wahrhaftig, C. 1965. Physiographic divisions of Alaska. U.S. Geological Survey, Professional Paper 482.

Weber, F.R., Foster, H.F., Keith, T.E.C., and Dusel-Bacon, C. 1978. Preliminary geologic map of the Big Delta quadrangle, Alaska. U.S. Geological Survey, Open-File Report 78-529-A, scale 1 : 250 000.

Wilson, F.H., Smith, J.G., and Shew, N. 1985. Review of radiometric

data from the Yukon crystalline terrane, Alaska and Yukon Territory. *Canadian Journal of Earth Sciences*, **22**: 525–537.

Zhang, L.-S., Shärer, U. 1996. Inherited Pb components in magmatic titanite and their consequence for the interpretation of U–Pb ages. *Earth and Planetary Science Letters*, **138**: 57–65.

See Appendix on the following page

## Appendix A

**Table A1.** Summary of field and petrographic data for  $^{40}\text{Ar}/^{39}\text{Ar}$  samples.

I.D. No.	Sample No.	Latitude, longitude	Quad.	Rock type (mineral dated)
1	83ADb4H	63°08'37", 142°00'00"	Eagle A-2	Qtz monzonite (Hbl, Bt)
2	91ADb10	64°10'09", 141°33'32"	Eagle A-2	Hbl monzonite (Hbl)
3	98ADb30	64°20'07", 141°50'36"	Eagle B-2	Hbl-Cpx monzodiorite (Hbl)
4	98ADb2C	64°25'08", 141°22'45"	Eagle B-1	Ms quartzite – exhalite with banded sulfides (Ms)
5	91ADb11A	64°13'24", 142°20'20"	Eagle A-3	Grt Qtz mica schist (Bt)
6	93ADb21A	64°12'56", 142°14'32"	Eagle A-3	Hbl-Bt-Grt schist (Bt)
7	91ADb4A	64°12'07", 141°20'36"	Eagle A-1	Grt-St Qtz mica schist (Bt)

Field description and available dating information	Petrography <sup>a, b, c</sup>
Medium-grained Bt–Hbl Qtz monzonite. Forms 30 ft (1 ft = 0.3048 m) high tor with gently dipping joint planes. Hbl appears to be more abundant than Bt locally; Hbl up to 0.5 cm but generally about 3 mm. A few felsic fine-grained aplitic rocks locally cut the Bt–Hbl rock.	Kfs, Pl, Qtz, Hbl, Bt, Ttn, Opq, Ap, Zrn. Hypidiomorphic granular; a small percentage of grains exhibit very minor alteration of Bt to Chl, and Hbl to Bt; Ksp and Pl in ~ equal amounts; Qtz makes up ~5–10% of rock and has undulose extinction.
Sample collected from large block from rubble pile of fresh, medium-grained Hbl-bearing plutonic rock. Rock contains mafic segregations, which are coarse grained (a few cm × ~1 cm). Slight suggestion of an igneous foliation. Ttn gives a U–Pb age of 189.6 ± 0.5 Ma (J.K. Mortensen, written communication)	Medium-grained Pl–Kfs–Hbl monzonite; Qtz < 5 %; trace amounts of Opq, Ttn, myrmekite, and sparsely developed secondary Chl from Hbl and Ep from Pl; alignment of elongate Pl and Hbl crystals suggests a magmatic foliation. Qtz has weakly developed undulose extinction and mostly straight grain boundaries.
Sample collected from flat area of slab rubble crop ~50 m south of main tor. Pegmatite and aplite dikes up to 15 cm thick occur locally. Sample from batholith informally called the “Pig pluton” because its outcrop pattern (Foster 1976) resembles the shape of a Pig’s head.	Medium-grained Pl–Hbl–Cpx monzodiorite; Dark green Hbl up to 2 mm in length; some Cpx rimmed by Hbl; Qtz < 5 %; minor amount of anhedral, interstitial Ep along some Hbl margins (associated with partly altered Fld); minor Bt associated with or after Hbl; very minor Kfs; trace of Ap. Hypidiomorphic granular texture.
Sample from slab of rusty weathering, light-tan Ms quartzite with bands of sphalerite and galena; these rusty rocks occur in patches within a large borrow pit composed primarily of dark gray carbonaceous quartzite.	Qtz–Ms quartzite with abundant honey-colored sphalerite, dark grey galena, scattered euhedral to subhedral pyrite cubes, and a minor amount of very fine-grained prismatic celsian. The presence of sulfides and barium Fld (celsian) is consistent with an exhalative origin for the Qtz-rich sulfide-bearing layers. Qtz has undulose extinction and irregular grain boundaries.
Sample collected from top of 2 m high outcrop of Grt–Bt schist. Scattered 1–2 cm long Bt crystals are randomly oriented on the foliation surface, imparting a garbenschiefer texture. Garnetiferous Qtz–Bt schist–gneiss with Grt up to 6 mm crops out nearby.	Medium-grained garnetiferous Bt–Qtz–Ms schist; trace amounts of Pl and Ilm. Grt porphyroblasts reach 2.5 mm in size and helicitically enclose rotated Qtz folia; Bt occurs both as thin, ~1 mm-long grains, that, together with Ms and Qtz, define the foliation, and as grains coarser, 2–3 mm-long blades at a slight angle to the foliation; Ms is present in discrete folia that show alteration to finer grained Ser. Most Qtz grains have uniform extinction and straight grain boundaries.
Outcrop of compositionally variable Grt–Qtz–Bt–Hbl schist; Grt reaches > 1 cm.	Medium-grained unaltered bluish green Hbl and brownish green Bt, and fine-grained weakly kaolinitized, untwinned Pl, and Qtz; minor Grt, Ilm, Zo, and Ep; 0.7-mm-long Grt porphyroblast has “fishnet” texture composed of trains of Grt that are separated by foliation-parallel Qtz. Qtz has uniform extinction and most grains have some straight grain boundaries. A compositionally similar schist from same field station contains retrograde Chl around Grt rims and from Bt, but Hbl appears unaltered. Qtz is fine-grained, has straight grain boundaries, and exhibits either uniform extinction or weakly developed undulose extinction.
Outcrop of garnetiferous St-bearing Qtz–Ms–Bt schist; Ky occurs in other layers in the outcrop and Stp locally occurs in cross-cutting cleavages or fractures.	Medium-grained Bt (dark brown to tan)–Ms–Qtz schist with abundant 2-mm porphyroblasts of Grt and St; minor Kfs and Opq; very minor, local alteration of Grt and Bt to Chl; lepidoblastic, porphyroblastic texture. Most Qtz grains have weakly developed patchy/undulose extinction but some have uniform extinction and straight grain boundaries.

**Table A1** (continued).

I.D. No.	Sample No.	Latitude, longitude	Quad.	Rock type (mineral dated)
8	98ADb16	64°11'45", 141°23'21"	Eagle A-1	Mylonitic Bt augen gneiss (Bt)
9	91ADb3	63°59'31", 141°17'14"	Tanacross D-1	Hbl schist (Hbl)
10	90ET11	63°56'32", 141°03'34"	Tanacross D-1	Grt amphibolite (Hbl)
11	90ADb8A	63°54'51", 141°00'19"	Tanacross D-1	Qtz-Zo-Bt-Ms gneiss (Ms, Bt)
12	90ADb17A	63°51'58", 141°30'34"	Tanacross D-2	Hbl-Bt-Ky-Grt schist (Bt)
13	83ADb23	63°49'00", 141°37'08"	Tanacross D-2	Amphibolite (Hbl)
14	90ADb23B	63°50'16", 141°32'47"	Tanacross D-2	Grt-Qtz-Amp schist (Hbl)
15	90ADb24	63°50'11", 141°32'07"	Tanacross D-2	Ms-Bt augen gneiss (Ms)

Field description and available dating information	Petrography <i>a, b, c</i>
Sample from slab of coarse augen gneiss with pink Kfs augen 1–2 cm in length.	Qtz–Bt–Kfs blastomylonitic gneiss. Bimodal grain size with very fine-grained domains parallel to foliation that are composed of 0.1 mm crystals of annealed Kfs. Coarser-grained oval patches (augen) and bands (former veins?) are composed of aggregates of individual Qtz crystals 1 mm in length. 0.3 mm-long olive-brown Bt forms narrow folia. Qtz grains have ragged margins and strongly developed undulose extinction.
Sample of dark green, calcareous Hbl–Bt–Chl–Pl schist from a large train-sized tor. Sample is from a ~20 cm-thick, coarse-grained layer that is interlayered with finer grained Bt–Wm ± Grt schist that makes up the rest of the outcrop; rocks are highly sheared.	Medium-grained Act–Bt–Chl–Cal–Pl schist; pale-green, 2–5-mm long, Act porphyroblasts form augen-like clasts that are surrounded by through-going wavy folia of elongate Chl, equant Cal, sericitized Pl, and locally chloritized Bt, indicating shearing under greenschist-facies conditions. Trace amount of Qtz with weakly developed undulose extinction and both straight and irregular grain boundaries.
Outcrop of Grt amphibolite.	Medium-grained, fresh, garnetiferous Hbl schist with minor amounts of Pl, Ttn, and Zo, and trace amounts of Qtz and Opq; nematoblastic, porphyroblastic texture with 1–2-mm porphyroblasts of Grt. Qtz has undulose extinction and mostly straight grain boundaries.
Outcrop of strongly mylonitized, interlayered Qtz-rich schist and feldspathic gneiss; 80 meters to west, Grt amphibolite forms a ~30 m-thick layer within the schist and gneiss sequence.	Medium-grained Qtz–Zo–Bt–Ms–Pl–Kfs mylonitic gneiss; Qtz is highly fractured; Qtz, Ms, and Bt all have undulose extinction.
Sample of garnetiferous Hbl–Bt–Ky schist collected from 50 ft. exposed section of interlayered schist and Grt amphibolite. Schist contains abundant prisms of turquoise Ky, pale green Hbl, and euhedral 0.5 cm Grt. P-T determinations for Grt amphibolite from this locality and another 200 meters away indicate peak metamorphic conditions of 6.5–8.8 kbar, 520–560°C and 10.8–11.7 kbar, 595–635°C, respectively, (Dusel-Bacon et al. 1995).	Medium-grained matrix of Qtz and golden-tan Bt enclose porphyroblasts of pale bluish-green to tan Hbl, euhedral Grt and Ky. Grt poikilitically encloses abundant Qtz inclusions which, in one porphyroblast, lie at an angle to the main fabric and thus may be indicative of an earlier fabric or may simply indicate rotation of the Grt during growth. Minor phases include Ilm and Rt. Retrogressive alteration of the schist varies from negligible to extreme, characterized by ubiquitous partial alteration of Hbl, Bt, and Grt to Chl and Ky to Ser.
Outcrop of schistose amphibolite and Bt–Hbl–Fld schist that occurs within a large body of highly deformed augen gneiss.	No thin section available.
Layer of homogeneous amphibole schist with rusty-weathering sulfides; layers of St–Grt–Bt–Ms–Qtz schist crop out nearby.	Medium-grained Qtz–Amp schist with minor amounts of 1.5 mm Grt, Chl, Pl, and Opq; Amp crystals are exceptionally fresh; nematoblastic texture; a lower amphibolite-facies metamorphic grade is suggested by the pale green color of Amp and small size of Grt in this rock and the presence of poorly formed trains of St in nearby rocks. Qtz has weakly developed undulose extinction and mostly straight grain boundaries.
Rubble crop of well foliated Ms–Bt augen gneiss with well-developed S-C fabric. A ~360 Ma crystallization age for the igneous protolith is indicated by concordant Zrn U–Pb ion probe (SHRIMP) data (Heslop et al. 1995; I. Williams and C. Dusel-Bacon, unpublished data).	Medium-grained Ms–Kfs–Qtz augen orthogneiss, with minor fine-grained Bt (locally altered to Chl and Fe–Ti oxides) and Pl; Kfs is slightly kaolinitized. Well-developed flaser fabric in which Qtz is strained and polygonized.

**Table A1** (*continued*).

I.D. No.	Sample No.	Latitude, longitude	Quad.	Rock type (mineral dated)
16	90ADb12	63°54'30", 141°49'45"	Tanacross D-2	Ms–Bt augen gneiss (Ms, Bt)
17	90ADb2E	63°49'52", 141°18'57"	Tanacross D-1	Bt–Ms augen gn (Ms, Bt)
18	90ADb6B	63°46'35", 141°06'12"	Tanacross D-1	Bt–Hbl augen gneiss (Bt)
19	91ADb26	64°14'03", 143°38'12"	Eagle A-6	Bt–Hbl Qtz monzonite (Bt)
20	91ADb35	64°09'04", 143°07'36"	Eagle A-5	Qtz monzonite (Hbl)
21	91ADb25	64°11'34", 143°40'00"	Eagle A-6	Qtz mica schist (Ms)
22	91ADb28A	64°12'05", 143°32'32"	Eagle A-6	Grt–Chl–Wm–Qtz schist (Ms)
23	91ADb37	64°02'29", 143°22'36"	Eagle A-5	Hbl–Ep–Qtz schist (Hbl)

Field description and available dating information	Petrography <i>a, b, c</i>
Intensely deformed outcrops of augen gneiss with highly elongated white Kfs megacrysts up to 12 cm long; well-developed s-c fabric indicates top-to-the northwest ductile shear; later crenulations and asymmetric folds (1 cm–0.5 m amplitude) indicate top-to-the southeast shear under more brittle conditions.	Ms–Kfs–Qtz–Bt ortho augen gneiss; Ms occurs in folia of pristine small prismatic books ~0.7 mm long; Bt forms thinner folia of more sheared, ragged grains that are locally altered to patches of Chl and needles of Rt. Kfs is generally kaolinitized and augen and matrix grains occur as a mosaic of tiny subhedral Kfs grains. Qtz grains exhibit a range of deformation from moderate to weak undulose extinction; some Qtz forms eye-shaped mosaics that are coarser than the individual grains in the Kfs mosaics.
Sample collected from a 50-m thick sill(?) of augen gneiss that occurs within a pelitic sequence of garnetiferous Qtz–Fld–Bt–Ms–Chl schist. Augen of Kfs within the gneiss reach up to 2.5 cm in length, and Grt within the pelitic schist reach 1 cm in diameter.	Qtz–Kfs–Bt–Ms–Pl ortho augen gneiss; minor amount of granules or poorly formed porphyroblasts of Grt and trace amounts of Chl, Zrn, Opq, and Ap; Bt and Ms very fresh; blastomylonitic, porphyroclastic texture. Qtz has mostly uniform extinction and straight subgrain and grain boundaries but weak patchy–undulose extinction preserved in some grains.
Bt–Hbl augen gneiss with pin-head-sized garnets; contains well-developed lineation but poorly developed foliation. A $353 \pm 4$ Ma crystallization age for the igneous protolith is indicated by nearly concordant U–Pb Zrn ages; Ttn gives a $^{206}\text{Pb}/^{238}\text{U}$ age of ~135 Ma (Dusel-Bacon and Aleinikoff 1996).	Pl–Kfs–Bt–Qtz ortho augen gneiss with minor amounts of green prismatic Hbl, 0.5-mm Grt granules, clusters of Ttn prisms, and trace amounts of zircon and opaque minerals; augen are generally composed of poikilitic Kfs with Qtz inclusions and myrmekitic margins, but locally consist of aggregates of 1 mm-size grains of Pl, Qtz, and Kfs; lepidoblastic to mylonitic, porphyroclastic texture. Qtz has weakly developed undulose extinction and both straight and irregular grain boundaries.
Sample of Bt–Hbl Qtz monzonite from slab in coarse rubble, collected near summit 4812 feet.	Fine-grained Kfs–Pl–Bt–Hbl monzonite. Qtz ~10% and trace amounts of Opq and Ap. Largest and most euhedral Bt is dark brown; finer grained brown Bt is locally altered to green Bt along cleavage planes and around grain margins; Hbl forms bright green irregular-shaped masses that are commonly altered to Ep or green Bt; Fld shows patchy kaolinitization. Qtz has uniform or weakly undulose extinction.
Hbl Qtz monzonite from angular, blocky rubble pile; part of Mt. Veta pluton; 188 Ma $^{40}\text{Ar}/^{39}\text{Ar}$ Hbl age determined by Cushing (1984). Ttn gives a U–Pb age of $185.4 \pm 1.4$ Ma (J.K. Mortensen, written communication)	Coarse-grained Pl–Kfs–Hbl Qtz monzonite. Qtz makes up ~10% of rock and euhedral Ttn, myrmekite, and patches of coarse, polycrystalline Cal are present in trace amounts. Hbl is green and exceptionally fresh; alteration of some Pl grains to Ser and in a few grains of Hbl to Chl. Hypidiomorphic granular texture. Qtz has weakly undulose or, less commonly, uniform extinction.
Sample of Pl–Qtz–Ms–Bt gneissic schist collected from 5-m-high outcrop; 2 linear tor outcrops occur lower down on the same slope.	Medium-grained Bt–Ms–Qtz–Pl schist; Bt (reddish-brown in color) and Ms very fresh; lepidoblastic texture. Qtz has undulose extinction and ragged grain and subgrain boundaries.
Sample of fine-grained Chl–Wm quartzite–schist collected from outcrop; underlain by Chl–Wm schist with retrograded (chloritized) ~4-mm Grt; Chl books form lineation which suggests they may have formed during later Chl-grade event.	Fine-grained Qtz–Wm schist with medium-grained (up to 3 mm-long) tabular Chl grains and 1-mm diameter skeletal Grt; Chl and Wm porphyroblasts occur both parallel to the foliation and at an angle to it; Qtz has undulose extinction and ragged subgrain boundaries; some Qtz grains form small augen.
Outcrop of coarse to medium-grained Hbl–Ep–Qtz schist.	Medium-grained Hbl schist dominated by Hbl grains up to 3 mm in length. Some of the larger Hbl porphyroblasts have cores full of finely crystalline to dusty Ilm. Minor Fld, Ep, Zo, Qtz, Rt, Ttn, and Ilm. Some Fe-staining in cracks. Qtz has undulose extinction and most subgrain boundaries are straight.

**Table A1** (*concluded*).

I.D. No.	Sample No.	Latitude, longitude	Quad.	Rock type (mineral dated)
24	91ADb36A	64°05'47", 143°13'34"	Eagle A-5	Ms–Qtz schist (Ms)
25	91ADb36D	64°05'47", 143°13'34"	Eagle A-5	Grt amphibolite (Hbl)
26	91ADb31A	64°11'01", 143°25'03"	Eagle A-5	Ms–Qtz–Grt–Zo–Chl schist (Ms)
27	79AFr4024J	64°23'13", 144°37'48"	Big Delta B-2	Amphibolite (Hbl)
28	80AFr115D	64°17'53", 144°38'59"	Big Delta B-2	Grt amphibolite (Hbl)
29	87ANk66A	64°17'54", 144°38'48"	Big Delta B-2	Hbl–Pl schist (Hbl)
30	91ADb21C	64°10'25", 144°15'40"	Big Delta A-1	Amphibolite (Hbl)
33	87ANk35A	64°36'09", 145°18'11"	Big Delta C-3	Hbl–Chl–Ttn–Pl schist (Hbl)
34	87APa55	64°39'40", 145°10'25"	Big Delta C-3	Qz–Ms schist (Ms)

<sup>a</sup>Mineral abbreviations are given in Table 1.

<sup>b</sup>Minerals listed in decreasing order of abundance.

<sup>c</sup>Grain-size criterion used: Fine-grained = 0.1–1 mm; medium-grained = >1–5 mm; coarse-grained = >5 mm.

Field description and available dating information	Petrography <i>a, b, c</i>
Outcrop composed of interlayered (top to bottom) Grt–Hbl gneiss (sample D), Grt–Bt schist in which garnets reach ~4 mm in diameter, and Ms–Qtz schist (sample A).	Medium-grained Ms–Qtz schist with euhedral, 2-mm long Ms books and elongate; many Qtz grains have straight contacts and uniform extinction, but others have weakly developed undulose extinction; minor amount of sericitized and kaolinitized Pl and Kfs. Although this sample shows only minor alteration of Fld, a sample of Bt–Grt gneiss from an adjacent layer shows intense retrograde alteration.
Outcrop of Ms–Grt–Zo–Chl Qtz schist; Grt ranges from 1–2 mm in diameter.	Medium-grained Hbl gneiss with bluish green, poikilitic Hbl, highly kaolinitized Pl, Qtz, Grt porphyroblasts (up to 2.5 mm), and trace amounts of Ilm. Most Qtz grains have undulose extinction, but some smaller grains have uniform extinction and straight grain boundaries. Inclusions in Hbl identified on electron microprobe as sodic Pl, Qtz, Ilm, Di, Bt, Ms, Chl, and minor Ttn.
Amphibolite forms a concordant layer, several tens of m-thick, within an area of quartzofeldspathic gneiss and semipelitic schist near the margin of a large body of augen orthogneiss.	Medium-grained garnetiferous Wm–Qtz schist with minor Zo and Chl (from Grt and rarely within Ms folia), and trace amounts of tourmaline prisms (up to 3.5 mm) and Ap needles. Most Qtz grains have undulose extinction and irregular grain boundaries.
Medium-grained Amp–Pl–Qtz–Grt gneiss. Infolded with associated rocks. Fld-rich segregations around Grt porphyroblasts.	Hbl, Pl, Ep, Ttn, Qtz, Rt. Nematoblastic; compositionally banded (white, Pl–Qtz-rich amphibolite and dark-green, dominantly Hbl, amphibolite) and folded. Qtz has weakly developed undulose extinction.
Outcrop of mafic schist; some layers have Grt porphyroblasts up to 5 mm in diameter.	Actinolitic Hbl, Pl, Qtz, Grt (irregular patches of granules; probably remnants of porphyroblasts now replaced, in part, by Pl), Rt (marginally altered to Ilm), Zrn. Nematoblastic, weak compositional banding. Qtz has undulose extinction and ragged subgrain boundaries.
Sample collected from outcrop of fresh amphibolite; amphibolite overlain by Grt amphibolite with Grt reaching 2 mm in diameter. Field location occurs at margin (base) of serpentized ultramafic body.	Medium-grained Hbl–Pl schist with minor Qtz, Chl, Ep, Zo, Ttn, and trace amount of Rt, commonly in cores of Ttn masses. Qtz has undulose extinction.
1 m thick layer of Hbl–Bt schist within exposure of Qtz–Kfs mica schist; both lithologies share same metamorphic fabric.	Medium-grained Hbl–Pl gneiss; minor amount of Ttn (clots of fine-grained rhombohedra) and Bt (elongate wisps present in some folia); trace amount of Qtz, which has undulose extinction.
	Fine-grained pale-green amphibole schist with abundant scattered Ttn grains and ragged, books of Chl or, less commonly, Ms, and a trace amount of Pl; a few Chl grains have Bt in their core, suggesting retrograde metamorphism of an originally higher temperature rock. Qtz has undulose extinction.
	No thin section available

